Accepted Manuscript

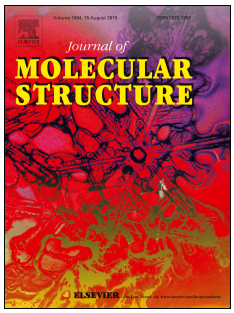

Structural, spectroscopic, electronic, nonlinear optical and thermodynamic properties of a synthesized Schiff base compound: A combined experimental and theoretical approach

Halil Gökce, Nuri Öztürk, Mehmet Kazıcı, Çiğdem Yörür Göreci, Serap Güneş

PII: S0022-2860(17)30132-1

DOI: 10.1016/j.molstruc.2017.01.089

Reference: MOLSTR 23394

To appear in: *Journal of Molecular Structure*

Received Date: 26 December 2016

Revised Date: 31 January 2017

Accepted Date: 31 January 2017

Please cite this article as: H. Gökce, N. Öztürk, M. Kazıcı, E. Yörür Göreci, S. Güneş, Structural, spectroscopic, electronic, nonlinear optical and thermodynamic properties of a synthesized Schiff base compound: A combined experimental and theoretical approach, *Journal of Molecular Structure* (2017), doi: 10.1016/j.molstruc.2017.01.089.

Graphical Abstract

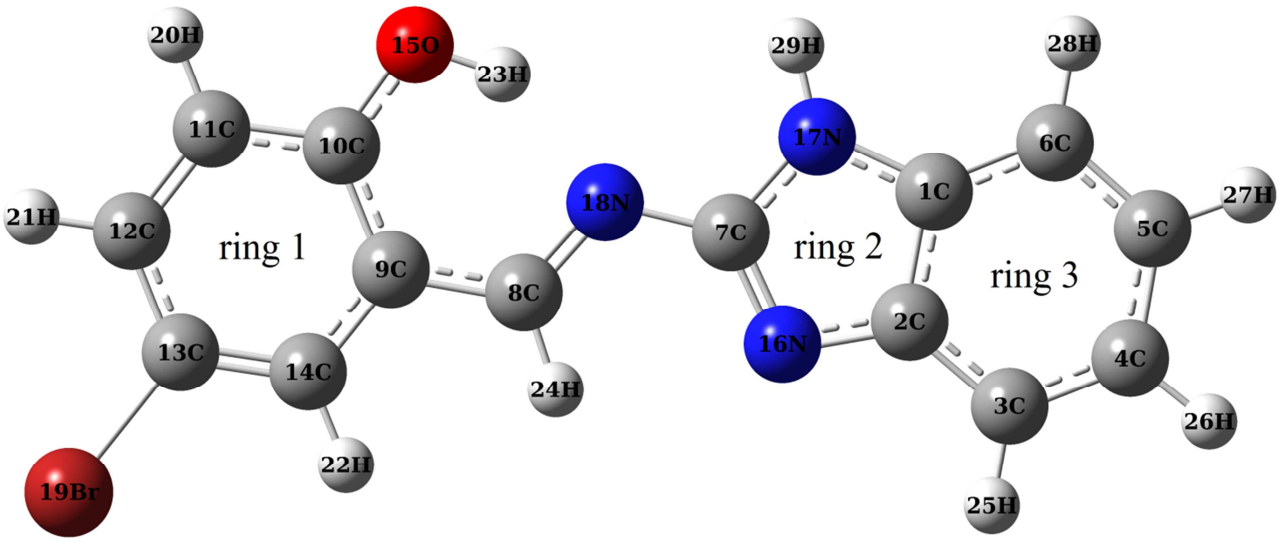

Structural, Spectroscopic, Electronic, Nonlinear Optical and Thermodynamic Properties of a Synthesized Schiff Base Compound: A Combined Experimental and Theoretical Approach

Halil Gökce[1*], Nuri Öztürk[2], Mehmet Kazıcı[3,4], Çiğdem Yörür Göreci[5], Serap Güneş[3]

[1] *Vocational School of Health Services, Giresun University, 28100, Giresun, Turkey*

[2] *Dereli Vocational School, Giresun University, 28950, Giresun, Turkey*

[3] *Yıldız Technical University, Faculty of Arts and Science, Department of Physics, Davutpasa Campus, 34210, Esenler, Istanbul, Turkey*

[4] *Siirt University, Faculty of Arts and Science, Department of Physics, 56100, Siirt, Turkey*

[5] *Yıldız Technical University, Faculty of Arts and Science, Department of Chemistry, Davutpasa Campus, 34210, Esenler, Istanbul, Turkey*

ASchiff base compound, 2-[(1*H*-benzimidazol-2-ylimino)methyl]-4-bromophenol (**BISB**), was synthesized and its spectroscopic characterizationwas performed using experimental methodssuch as FT-IR, Raman, proton and carbon-13 NMR chemical shifts and UV-Vis. spectroscopies.Density functional theory (DFT/B3LYP/6-311G(d,p)) computations were used to investigatethe optimized molecular geometry, conformational forms, harmonic vibrational wavenumbers, NMR chemical shifts, UV-Vis. spectroscopic parameters, natural bond orbital (NBO) analysis, HOMO-LUMO energies, nonlinear optical (NLO) properties, molecular electrostatic potential (MEP) map, atomic charges and thermodynamic properties of the **BISB** molecule. The assignments of vibrational modes wereperformed by means of potential energy distribution (PED) using VEDA4 program. The NBO analysis was used to investigate intramolecular hyrogen bonding (O-H···N), bond species, hyperconjugation interactions and intramolecular charge transfers (ICTs). Considering the computed HOMO and LUMO energies, the quantum molecular descriptors such as ionization potential (I), electron affinity (A), chemical hardness (η), chemical softness (ζ), electronegativity (χ), chemical potential (μ) and electrophilicity index (ω) parameterswere investigated for the **BISB** molecule. DFT computations were also performed to determine the dipole moment (μ), the mean polarizability (α), the anisotropy of the polarizability ($\Delta\alpha$) and the first hyperpolarizability (β_0) values. The recorded experimental spectroscopic results are in a good harmony with the computed data.

Keywords: Vibrational spectroscopy, NMR chemical shifts, Electronic properties, DFT computations, NLO analysis, Thermodynamic properties

[*] Corresponding Author E-mail: halil.gokce@giresun.edu.tr, halilgokce.hg@gmail.com

1. Introduction

Benzimidazoles which are members of heterocyclic compoundsconsist of the combination of benzene ring and the imidazole ring having nitrogen heteroatom.The benzimidazoles also have special significance due to their molecular arrangement with heteroaromatic and homoaromatic parts. The different substitutions on rings and their derivatives provide additional features such as functionality andenable easy modification of the electronic characteristics [1].Benzimidazole and its derivatives have important functions with many pharmacological and biological activities such as antiviral, antidiabetic and antitubercular, anticancer, antimicrobial, antioxidant, anti-hepatitis-C-virus, antihistaminic, antiallergic etc. [2-6].

Also, Schiff bases known as azomethines or imines are also a crucialclass of organic compounds because of their applications in many fields including biological, inorganic and physical applications [7]. Properties of the benzimidazole molecule with Schiff baseswhen assembled in a molecule skeleton, the structure characteristics are carried to a higher level [8,9].

In this study, we present molecular properties such as vibrational spectra (FT-IR and Raman), proton and carbon-13 NMR chemical shifts, UV-Vis. spectral parameters, molecular geometric parameters, HOMO and LUMO peroperties, quantum molecular descriptors, atomic charges, NBO analysis, NLO roperties, MEP surface and thermodynamic properties of 2-[(1H-benzimidazol-2-yl)iminomethyl]-4-bromophenol (**BISB**) molecule. Detailed analyses of structural, spectroscopic, magnetic, electronic, optical and thetmodynamic propertiesof the **BISB** molecule are not available in the literature. The quantum chemical investigations were performed by means of DFT/B3LYP method with the 6-311G(d,p) basis set, for the first time. The quantum chemical computations have been widely used to determine the structural, spectroscopic, magnetic, electronic, optical and thermodynamic properties of molecular systems, without experimental data. Additionally, the quantum chemical computations provides a powerful support for experimental studies.

2. Experimental

The condensation reaction was performed under the inert atmosphere of nitrogen. Ethanol was purified and dried according to standard procedure. 5-Bromo-2-hydroxybenzaldehyde and 2-Aminobenzimidazole (Merck) were used as purchased.

2.1.Physical Measurements

Melting points were obtained with a Gallenkamp Melting point apparatus in open capillaries. The absorption spectra were recorded on an Agilent 8453 UV-Vis spectrometer that is the spectral bandwidth of 1 nm. The UV-Vis. spectrum of 2-[(1*H*-benzimidazol-2-ylimino)methyl]-4-bromophenol was recorded in chloroformusing quartzcell 1 cm.

The IR (ATR) spectrum was recorded at the room temperature on a Perkin Elmer Spectrum One Bv 5.0 spectrophotometer at the interval of 4000-400 cm^{-1}a resolution of 4 cm^{-1}.^{1}H and ^{13}C NMR chemical shifts were recorded on a Bruker 500 MHz ($CDCl_3$) spectrometer. Chemical shifts (ppm) were referenced to the internal standard tetramethylsilane (TMS). Mass spectra (LC-MS) were determined on a Agilent 1200 Infinity HPLC and Agilent 6460 Jet-Stream TripleQuad spectrometer (350°C and 11L/min). Raman spectrum was measured with the Bruker Optics FT-Raman Scope III System (an air-cooled 1064 nm Nd:YAG laserexcitation source) in the region of 4000-100 cm^{-1}. Resolution and accumulation (scan number) for Raman spectrum are 4 cm^{-1} and 100 scans, respectively. The reactions were monitored by thin layer chromatography (TLC).

2.2. Synthesis of Schiff Base Ligand (BISB)

2-[(1*H*-benzimidazol-2-ylimino)methyl]-4-bromophenol [10], 5-bromo-2-hydroxybenzaldehyde (0.201 g, 1 mmol) was added to the 2-aminobenzimidazole (0.133 g, 1 mmol) in 10 mL absolute ethanol. Reaction mixture was stirred at reflux temperature for 6 h, under nitrogen atmosphere. The resulting solution was reduced to approximately 1/2 of its volume by rotary evaporation. The product precipitate was in pale orange solid form. The solid was filtered off, washed with ethanol and recrystallized from chloroform/ hexane (1:1) mixture and dried under vacuum. Yield: 86%. Orange crystals. m.p. 248°C; UV-vis: λ_{max} (nm)= 386. IR (ATR-IR): ν(cm^{-1}): 3317, 3068, 1620. ^{1}H NMR (DMSO-d_6, 500 MHz): δ (ppm)= 12.81 (s, 1H), 12.03 (s, 1H), 9.63 (s, 1H), 8.09-7.01 (m, 7H). LC-MS: *m/z* = 316 $[M]^+$ ($C_{14}H_{10}BrN_3O$).

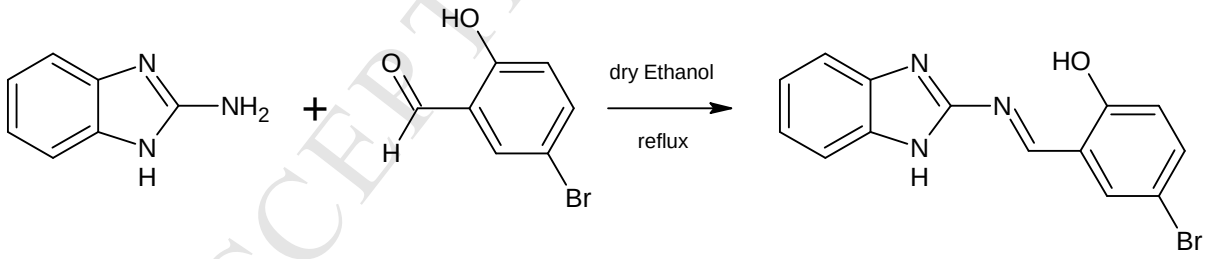

BISB

Scheme 1. Preparation of Schiff base **BISB**.

3. Computational Details

DFT computations of molecular geometry, IR wavenumbers, proton and carbon-13 NMR chemical shifts (in vacuum and DMSO), UV-Vis. spectroscopic parameters (in vacuum and chloroform), NBO analysis, NLO properties, atomic charges, MEP surface, FMOs analyses and thermodynamic parameters of the **BISB** molecule were doneusingGaussian 09W program package [11]. The calculated results were visualized by via GauusView5 program [12].

All computations were performed using DFT (Density Functional Theory)/B3LYP (Becke's three parameter exact exchange-functional (B3) combined with gradient-corrected correlational functional of Lee, Yang, Parr (LYP)) method with the 6-311G(d,p) basis set [13,14]. The computedharmonicvibrational wavenumbers were scaled with 0.967 for B3LYP/6-311G(d,p) level [15]. The detailed vibrational assignments were performed on basis of potential energy distribution (PED) analysis using VEDA 4 program[16].For ^{1}H and ^{13}C NMR isotropic chemical shift calculations, the optimized molecular geometries of the **BISB**molecule were first obtained at B3LYP/6-311G(d,p) level in vacuum and DMSO using integral equation formalism polarizable continuum model (IEFPCM). Then, ^{1}H and ^{13}C NMR chemical shifts of the **BISB** molecule were performed usingaforementioned computational level and solventswith gauge invariant atomic orbital (GIAO) approach [17-19].The UV-Vis. calculations of the **BISB** molecule were doneusing TD-DFT method in vacuum and chloroform. The HOMO and LUMO energy values and their shapes were simulated using B3LYP/6-311G(d,p) level. According to the computed HOMO and LUMO energy values of the **BISB** molecule, the some molecular properties such as ionization potential (I), electron affinity (A), chemical hardness (η), chemical softness (ζ), electronegativity (χ), chemical potential (μ) and electrophilicity index (ω)werecomputed.The nonlinear optical (NLO) properties such as the dipole moment (μ), the mean polarizability (α_{total}), the anisotropy of the polarizability ($\Delta\alpha$) andthe first hyperpolarizability (β_0) were performedwith thementioned computational level. The NBO analysis was done to understandthe interactions among bonds and intramolecular charge transfers (ICTs) or hyperconjugative interactions in the **BISB** molecule. The molecular electrostatic potential (MEP) and its contours surfaces was simulatedusing the optimized molecular geometryof the **BISB** molecule.Finally, the atomic charges (Mulliken, APT and NBO)and thermodynamic properties (termal energy (E), heat capacity (C_v), entropy (S), etc.) were computed using B3LYP/6-311G(d,p) level.

4. Results and Discussion

4.1. Conformational Analysis and Molecular Structure

The optimized molecular structure with B3LYP/6-311G(d,p) level of the 2-[(1*H*-benzimidazol-2-ylimino)methyl]-4-bromophenolis given in Fig. 1. The computed molecular geometric parameters (bond lengths and bond angles) are summarized in Table 1. In the literature, the experimental structural parameters, obtained with single crystal X-Ray analysis, are not available for the **BISB** molecule. However,Liu et al. [20] recorded the molecular geometry and structural parameters of 2-[(1H-benzimidazol-2-yl)iminomethyl]-4,6-dibromophenol ethanol hemisolvate compound, which belongs to a similar structure with the **BISB** molecule, using experimental single crystal X-Ray method. The computed root mean square deviation (RMSD) and

linear correlation coefficients(R^2) values for the conformer 1 were obtained as 0.088Å and 0.96979 (for the experimental and computed bond lengths) and 0.965° and 0.97989 (for the experimental and computed bond angles), respectively.

The conformational analysis of the **BISB** molecule was performed for the C8-N18-C7-N16 torsion angle increasing by 2° steps from 0° to 180°. As a result of conformational analysis, the potential energy surface (PES) map obtained as a function of the C8-N18-C7-N16 dihedral angle is given in Fig. 2. According to Fig. 2, there are three conformational forms of the **BISB** molecule. These conformational forms are computed at 0.0° (Conformer 1), 166.0° (Conformer 2) and 104.0° (Conformer 3) values of the C8-N18-C7-N16 dihedral angle. The computed energy values for the conformer 1, conformer 2 and conformer 3 are -3353.34936242 a.u. (or 0.000 kcal/mol), -3353.34045992 a.u. (or 5.586 kcal/mol) and -3353.33645098 a.u. (or 8.102 kcal/mol), respectively. Considering the computed energy values for all conformational forms, we can say that the conformer 1 is the most stable state of the **BISB**molecule.The computed vibrationalwavenumbers with B3LYP/6-311G(d,p) level forthe conformer 1, conformer 2 and conformer 3 states of the **BISB** molecule are listed in Table 2. As seen from the calculated vibrational wavenumbers given in Table 2, the conformer 3 has one imaginary frequency. This situation shows that the conformer 3is the most unstable molecular geometryand itis a transition state.

The 2-[(1H-benzimidazol-2-ylimino)methyl]-4-bromophenol molecule wasformed by linking azomethine (R_1-CH=N-R_2) group of 4-bromophenol and 1*H*-benzimidazole groups. The C8-C9 bond length betweenthe azomethine and 4-bromophenol groups is computed as 1.443 Å. The C8=N18 bond length in the azomethine group of the **BISB** molecule is found as 1.298 Å. The C10-O15, C13-Br19, C14-C13-Br19, C9-C10-O15 and C10-O15-H23 bond parameters in the 4-bromophenol group of the **BISB** molecule are computed as 1.338 Å, 1.917 Å, 120.0°, 122.1° and 107.3°,respectively.The O15-H23, H23···N18,O15···N18 lengths and O15-H23···N18 angle as the intra-molecular hydrogen bonding parameters of the **BISB** molecule are calculated as 0.989 Å, 1.755 Å, 2.642 Å and 147.3°, respectively.In the literature, the C8-C9, C8=N18, C10-O15, C13-Br19, O15-H23, H23···N18, O15···N18 lengths and O15-H23···N18 anglewere experimentally recorded as 1.470 (6) Å, 1.268 (6) Å, 1.352 (6) Å, 1.891 (5) Å, 0.820 Å, 1.897 Å, 2.618 (5) Å, 146.0° for2-[(1H-benzimidazol-2-yl)iminomethyl]-4,6-dibromophenol ethanol hemisolvate molecule [20],1.452 (4) Å, 1.279 (4) Å, 1.350 (4) Å, 1.900 (4) Å, 0.825 Å, 1.830 Å, 2.586 (4) Å, 151.0° for2-[(*E*)-(5-amino-2,3-diphenylquinoxalin-6-yl)iminomethyl]-4-bromophenol one [21],1.440 (11) Å, 1.264 (10) Å, 1.371 (12) Å, 1.878 (9) Å, 0.820 Å, 1.890 Å, 2.609 (10) Å, 146.0° for (*E*)-4-bromo-2-[(4-ethylphenyl)iminomethyl] phenol [22] and 1.430 (7) Å, 1.290 (6) Å, 1.335 (5) Å, 1.887 (5) Å, 0.820 Å, 1.870 Å, 2.600 (6) Å 148.0°for2-[(1,3-benzothiazol-2-yl)iminomethyl]-4-bromophenol one [23], respectively.For 4-bromophenol, Jan et al. [24]obtained

the C-Br bond length as 1.919 Å, C-O length as 1.367 Å, O-H length as 0.963 Å, C-O-H bond angle as 110°, C-C-Br bond angleas 120.3° andC-C-O bond length as122.8° with B3LYP/6-311++G(d,p) level.The C7-N18 bond length between the azomethine and 1*H*-benzimidazole groups is computed as 1.383 Å. This bond length was computed as 1.401 (5) Å [20] and 1.396 (6) Å values in the literature. The C7=N16, C7-N17, C1-N17, C2-N16, N17-H29, N16-C7-N17, C2-N16-C7 and C1-N17-C7 bond parameters in the 1*H*-benzimidazole group werecomputed at 1.313 Å, 1.378 Å, 1.380 Å, 1.381 Å, 1.007 Å, 113.3°, 105.1° and 107.1° values, while they were recorded at 1.309 (5) Å, 1.342 (6) Å, 1.374 (5) Å, 1.381 (6) Å, 0.860 Å, 114.4 (4)°, 104.0 (4)° and 107.0 (4)° values for the 2-[(1H-benzimidazol-2-yl)iminomethyl]-4,6-dibromophenol ethanol hemisolvate molecule [20], respectively.Similarly, these bond parameters were experimentally obtained as 1.328 (2) Å, 1.364 (19) Å, 1.385 (2) Å, 1.391 (2) Å, 0.860, 112.7 (14)°, 104.9 (13)° and 107.3 (13)° for the 1,4-bis(1H-benzimidazol-2-yl)benzene methanol monosolvate molecule, respectively [25]. The C-C bond lengths in phenyl rings of the **BISB** molecule were computed at the interval 1.380 Å-1.421 Å, while the C-C-C bond angles are calculated between 116.8° and 122.5°. The C7-N18-C8, C9-C8-N18, C8-C9-C10 and N16-C7-N18 bond angles are found at 118.6°/120.3 (4)°, 122.1°/121.0 (4)°, 121.8°/121.4 (4)° and 128.5°/129.7 (4)°, respectively (calculated/experimental) [20].

4.2. Vibrational Frequency Analysis

There are 29 atoms and 81 vibrational modes of the 2-[(1*H*-benzimidazol-2-ylimino)methyl]-4-bromophenol molecule. The **BISB** moleculebelongs to C_s point group. The 81 vibrational modes are distributed as 55 A′ (in-plane vibrations) + 26 A″ (out-of-plane vibrations), under C_s symmetry. The measured and computed (unscaled and scaled) vibrational frequencies, IR intensities, Raman scattering activities, vibrational assignments and symmetry species of vibrational assignments are given in Table 2. The recorded (in solid phase) and simulated IR and Raman spectra of the **BISB** molecule are given in Fig. 3. The computed RMSD and R^2 values were obtained as 36.251cm^{-1}and 0.99767 (for the experimental and computed IR wavenumbers) and 9.904cm^{-1}and 0.99950 (for the experimental and computed Raman wavenumbers), respectively.

4.2.1. NH Vibrations

The absorption bands in the region of 3100-3700 cm^{-1}result fromthe presence of OH and NH stretching modes [26]. The observed band at 3317 cm^{-1} inexperimental IR spectra can be assigned to NH stretching vibrationof the**BISB** molecule. The computed wavenumber value for this band is 3536 cm^{-1}.The NH in-plane bending modes are observed at 1515 (IR)-1512 (R), 1367 (IR)-1378 (R), 1188 (IR)-1180 (R) and 1169 (IR)-1148 (R) cm^{-1} as associated with other vibrational bands, while the NH out-of-plane bending bands is found at 493 cm^{-1}(the computed at 482 cm^{-1} with 60%

contribution of PED) and 457 cm^{-1} (the calculated at 452 cm^{-1} with PED contribution of 25%) in Raman spectrum of the **BISB** molecule.

4.2.2. OH Vibrations

The OH vibration modes are very sensitive to hyrogen bonding interaction. Free OH stretching gives rise toa sharp band inthe regionof 3700-3500 cm^{-1} [41]. But, this band shifts to lower wavenumber under the presence of inter- and intra-molecular hydrogen bonding interactions and it is observed at the interval of 3200-3250 cm^{-1} [26,27]. Due to O-H···N intar-molecular hyrogen bonding interactions in the **BISB** molecule, the OH stretching band is observed at 3238 cm^{-1} in IR spectrum, while this band is computed at 3178 cm^{-1} with PED contribution of 99%. The in-plane and out-of-plane bending vibrations for the free OH group in phenol compounds lead to formation ofabsorption bands in the regions of 1330-1420 cm^{-1} and 650-770 cm^{-1}, respectively [28]. The OH in-plane and out-of-plane bending modesare shifted to high frequency region for the **BISB** molecule due to intramolecular O-H···N hydrogen bonding interaction. The OH in-plane bending vibrationsare found at 1599 (IR)-1605 (R), 1437 (IR)-1439 (IR) and 1401 (IR) cm^{-1}as mixed with other bands. The computed bands for OH in-plane mode are found at 1605 (19%), 1545 (17%), 1458 (20%), 1434 (14%) and 1404 (11%) cm^{-1}. Similarly, the OH out-of-plane bending vibration isfound at 783 (IR)-793 (R) $cm^{-1}$and it calculated at 787 $cm^{-1}$with 85% contribution of PED.

4.2.3. CH Vibrations

The CH stretching vibrations in aromatic compounds appear in the region 3000-3100 cm^{-1}. [26-29]. The observed band at 3068 cm^{-1} can be attributed to the CH stretching modes in aromatic rings of the**BISB** molecule. The CH stretching modes for aromatic groups are computed in the region of 3063-3100 cm^{-1}. The C_8-H_{24} stretching mode is observed at 3030 cm^{-1}, while this band is calculated at 2996 cm^{-1} with 100% contribution of PED.Additionally, the CH in-plane bending modes occur as mixed with other bands in the region of 1000-1600 cm^{-1}, while the CH out-of-plane bending (τHCCC or torsion CH) ones observe at the interval of 650-1000 cm^{-1} [26-29].The observed bands as coupled with other vibrations at 995 (IR)-1000 (R), 1074 (IR)-1080 (R), 1102 (IR), 1119 (R), 1137 (IR), 1204 (R), 1216 (IR), 1266 (IR)-1277 (R), 1301 (IR)-1308 (R), 1401 (IR), 1437 (IR)-1439 (R) and 1473 (IR) cm^{-1} can be attributed to the CH in-plane bending vibrations, while the CH out-of-plane bending bands are observed at 950 (R), 934 (IR), 872 (IR)-869 (R), 832 (R), 817 (IR)-817 (R) and 702 (IR)-692 (R) cm^{-1}.Likewise, the CH in-plane mode in azomethine gruop (-CH=N-) are found at1318 (IR)-1316 (R) cm^{-1} and it is computed at 1322 cm^{-1} with 29% contribution of PED. But, the CH out-of-plane bending band in this group is not observed in

experimental FT-IR and Raman spectra, whereas this band is calculated at 990 cm^{-1} with PED contribution of 91%.

4.2.4. CC, NC and OC Vibrations

The CC stretching vibrations of aromatic rings (skeletal vibration) usually occur in the interval of 1400-1650 cm^{-1} [30]. But, these bands can also be observed as combined with other vibrations below 1400 cm^{-1}. The CC stretching vibration modes in aromatic rings of the **BISB** molecule are listed in Table 2. The vibrational bands observed at 507 (IR)-511 (R), 603 (IR)-607 (R), 624 (IR), 643 (IR)-632 (R), 739 (IR)-737 (R), 848 (IR), 899 (IR) and 995 (IR)-1000 (R) $cm^{-1}$are assigned to the CCC in-plane bending vibration modes in aromatic rings of the **BISB**molecule. Similarly, the CCCC torsional modesin aromatic rings are given rise to absorption bands at 215 (R), 240 (R), 349 (R), 368 (R), 457 (R), 547 (IR)-527 (R), 570 (IR)-587 (R) and 752 (R) cm^{-1}.

The description of position in FT-IR and Raman spectra of NC stretching bands is very difficult due to the combining with several bands in fingerprint region [26]. The characteristic N=C stretching band for Schiff bases is observed in the region of 1600-1700 cm^{-1} [30-33]. But, this band can be shifted below 1600 cm^{-1} due to intra-molecular hydrogen bonding interaction. The azomethineN_{18}=C_8stretching band was observed at 1588 cm^{-1}in FT-IR spectrum as associated with other vibrational bands and it is computed at 1587 cm^{-1} with PED contibution of 38%. The obtained values are in good agreement with the literature [33]. Similarly, the stretching vibration mode for the other double bondN_{16}=C_7 is found at 1511 (IR)-1512 (R)/1495/14% and 1318 (IR)-1316 (R)/1322/14% cm^{-1} as combined with other bands (exp./cal./PED%) [34]. The stretching vibration modes of the single bond NC are observed at 1367 (IR)-1378 (R), 1340 (IR)-1337 (R), 1240 (R) and 1030 (IR)-1038 (R) cm^{-1}. The NC stretching vibration modes of the **BISB** molecule are listed in Table 2.

Silverstein and Webster [28] suggested that the OC stretching bands in phenol compounds it could be observed in the regions of 1390-1330 and 1260-1180 cm^{-1}.In this connection, the recorded strong band at 1266 (IR)-1277 (R) cm^{-1} can be assigned to OC stretching modes in phenol group of the **BISB** molecule [34]. The computed wavenumber value and PED contribution for this band are 1272 cm^{-1} and 35%, respectively. The in-plane bending vibrations between phenyl ring and OH group is found at 464 (IR)-467 (R) cm^{-1}/453 cm^{-1}/56%, whereas the out-of plane bending vibrations are obtained at 817 (IR)-817 (R) cm^{-1}/813 cm^{-1}/18%, 702 (IR)-692 (R) cm^{-1}/693 cm^{-1}/19% and 349 (R) cm^{-1}/332 cm^{-1}/18% as combined with other vibrational bands (exp./cal./PED).

4.2.5. CBr Vibrations

The CBr stretching mode appears in the region of 200-480 cm^{-1} [34,35]. Mooney [36-38] determined the position of vibrational modes for the C-X group (X=Cl, F, Br, I)in the frequency range of 1129-480 cm^{-1}. In this study, the CBr stretching mode is observed at 624 cm^{-1} in FT-IR spectrum and it is calculated at 617 cm^{-1} with PED contiribution of 13%. Additionally, the observed band at 302 cm^{-1} in Raman spectrum of the **BISB** molecule is assigned to CBr stretching mode and it is computed at 292 cm^{-1} with 29% contribution of PED. Likewise, the calculated band at 260 cm^{-1} with PED contiribution of 23% is identified as the CBr stretching mode. The CBr stretching, in-plane and out-plane bendings given in Table 2are ina good agreement with the obtained resultsfor the similar structures in literature [35-40].

4.3. Proton and Carbon-13 NMRChemical Shift Analyses

The NMR isotropic chemical shift analysis allows us to identify relative ionic species, to determined numbers of proton and carbon atoms and funtional groups in the molecular structure and to calculate reliable magnetic properties which provide accurate predictions of molecular geometries [41-44]. The experimental ^{1}H and ^{13}C NMR chemical shift spectra of the **BISB** molecule were recorded in DMSO-d_6 and they are given in Fig.4.The ^{1}H and ^{13}C NMR chemical shifts of the **BISB** moleculewere calculated at B3LYP/6-311G(d,p) level in vacuum and DMSO solvent using IEFPCM solvent model. The experimentaland calculated NMR chemical shift values are listed in Table 3.The computed RMSD and R^2 values were obtained as 6.156 ppm and 0.97361 (in vacuum) and 6.312 ppm and 0.98031 (in chloroform) for the experimental and computed ^{13}C NMR chemical shifts, respectively.

The ^{13}C NMR chemical shifts were observed in the region of 110.57-163.12 ppm, while they are calculated at the interval of 121.82-168.40 ppm in vacuum and 122.23-168.37 ppm in DMSO for the **BISB** molecule.The C7, C8 and C10 atoms which are connected to the electronegative atoms are given carbon-13 NMR chemical shift signals at 153.86, 159.41 and 163.12 ppm, respectively. The chemical shift values of these atoms are higher than those of the other carbons in the **BISB** molecule.The calculated values for these carbon atoms are at 154.93, 167.69 and 168.40 ppm in vacuum and 156.18, 168.25 and 168.37 ppm in DMSO, respectively.Aromatic carbon atoms give resonance signals in the range of 100-150 ppm [41-44]. As expected, the NMR chemical shifts for aromatic carbon atoms are observed at the interval of 110.57-142.29 ppm, while they are computed at 111.51-147.65 ppm in vacuum and 114.04-147.22 ppm in DMSO.

Because of the intramolecular hyrogen bonding, the proton NMR chemical shift value of the H23 atom in phenolic groupisgiven rise toresonance signals at 12.81 and 12.03 ppm [28]. The computed value for H23 atom is 12.289 ppm in vacuum and 12.675 ppm in DMSO.The aromatic rings produce large deshielding effects and their π-bonding electrons act as a conductor and

chemical shift values for protons the bonded to carbon atoms in aromatic rings are observed in the region of 6-8 ppm [41-44]. The chemical shift values for NH proton in amide, pyrrole and indole groups give rise to resonance signals in the region of 5.00-8.50 ppm [28]. The H29 atom and proton atoms of aromatic rings in the **BISB** molecule were given signals at the interval of 7.01-8.09 ppm. The chemical shifts ofthe H29 atom and aromatic protonsarecalculated at 7.604/8.438 ppm and at the interval of 6.911-7.829/7.056-7.830 ppm (in vacuum/in DMSO), respectively. Likewise, the proton chemical shift signal for H24 atom is obtained at 9.63/9.761/9.708 ppm (exp./cal. in vacuum/cal. in DMSO).

4.4. Frontier Molecular Orbital Analyses

The highest occupied molecular orbital (HOMO) and the lowest unoccupied molecular orbital (LUMO) are called as the frontier molecule orbitals (FMOs) and they are the main orbitals taking part in chemical reactions [45]. The HOMO represents the outermost orbital filled by electrons. It is directly related to the ionization potential of the compound. Behaving as an electron donor, it can be considered as valance band of the system. The LUMO implies the first empty innermost orbital unfilled by electrons. It is directly related to the electron affinity. Behaving as an electron acceptor, it can be thought as conductance band of the system. The HOMO-LUMO energy band gap is an indication of molecular chemical stability. It is a very important parameter for determination of molecular electrical properties. Furthermore, the quantum molecular descriptors such as ionization potential,electron affinity, chemical reactivity, kinetic stability, polarizability, chemical hardness and softness, aromaticity and electronegativity can be found using HOMO-LUMO energy band gap [46]. The simulated HOMO-4, HOMO-3, HOMO-2, HOMO-1, HOMO, LUMO, LUMO+1, LUMO+2, LUMO+3 and LUMO+4 shapes and their energy values with B3LYP/6-311G(d,p) level are given in Fig. 5. The computed HOMO and LUMO energy values for the **BISB** molecule are found as -2.551 and -2.526 eV in vacuum and -6.069 and -6.086 eV in chloroform, respectively. The band gap between the HOMO and LUMO is obtained as 3.518 in vacuum and 3.559 eV in chloroform. The HOMO is mainly localized on whole molecule, while the LUMO ise mainly localized on other whole groups excluding Br atom. Both the HOMO and LUMO are mostly formed from the p-bonding and p-antibonding type molecule orbitals.

Considering the computed HOMO and LUMO energy values, the quantum molecular descriptors such as ionization potential, electron affinity, chemical hardness, softness, electronegativity and electrophilicity index parameters are summarized in Supplementary Table S1[46].

4.4. UV-Vis. Spectroscopic Analysis

The experimental UV-Vis. electronic absorption spectrumof the **BISB** molecule was recorded in the region of 200-600 nm in chloroform solvent. The simulated (in vacuum and chloroform) and experimental UV-Vis. electronic absorption spectra are given in Fig. 6. The experimental and computed UV-Vis. spectroscopic parameters and corresponding electronic transitionsare listed in Table 4.The strong absorption bands below 400 nm (in the region 350-390 nm) in experimental UV-Vis. spectrum of Schiff base compounds indicateenol-imine form of the structure under investigation. These strong absorption bands in this region can be attributed to π→π* transition that is resulted from azomethine and aromatic groups. In this connection, the strong absorption wavelengths observed at 386 and 353 nm in the experimental UV-Vis. spectrum can be assigned to π→π* electronic transition in the **BISB** molecule. The calculated values corresponding to these experimental bands are at 387.09/394.45 nm and 341.80/341.98, respectively (in vacumm/in chloroform). As known, the most possible electronic transition in a molecule is from HOMO to LUMO. Therefore, the highest oscillator strength and major transitioncorresponding to strong wavelength at 387/387.09/394.45 nm (exp. in chloroform/cal. in vacuum/cal. in chloroform) in UV-Vis. spectra of the **BISB** molecule are computed as 0.68732/0.69817 and H→L, respectively.The recorded absorption wavelength at 278 nm is assigned as π→π* electronic transition which is resulted from aromatic groups (4-romophenol and 1*H*-benzimidazole) in the **BISB** molecule.The electronic absorption wavelength observed at 245 nm can be assigned to n→σ* and this band confirms intramolecular hydrogen bonding interaction (O-H···N) in the **BISB** molecule.The other higher oscillator strength value and its major contribution in simulated UV-Vis. spectra are obtained as 0.3288/0.3478 and H-1→L+2 for wavelengths of 216.47/217.49 nm, respectively

4.5. NBO Analysis

The NBO analysis is a powerful method to determine intra- and inter-molecular bonding interactions, bond species, bond structures and natural atomic charges in the molecular systems.Besides, it is used to investigate hyperconjugation interactions or charge transfers (ICT) and the stability between Lewis type (bonding or lone pair) filled orbitals and non-Lewis type (antibonding or Rydgberg) vacancy orbitals. The hyperconjugative interaction energy (or the stabilization energy, *E*(2)) shows the interaction between donor and acceptor groups. Delocalization of electron density between occupied Lewis type orbitals and formally unoccupied non-Lewis orbitals correspond to a stabilizing donor-acceptor interaction[47].

The NBO data computed at B3LYP/6-311G(d,p) level are given in Table 5.The strong hyperconjugation interactions or intramolecular charge transfers (ICTs) were computed between σ and π bonding electrons of the C-N, C-C and C-H bonds and σ* and π* antibonding ones of C-C, C-N, C-H, N-H, O-H andC-Br ones. In addition, other strong hyperconjugation interactions are also

foundbetween the lone pair n electrons of O, N and Br atoms and σ* and π* antibonding ones of C-C, C-N, C-H and O-H bonds. The stabilization energy values greater than 4 kcal mol^{-1} are summarized in Table 5. The π bond electrons are weaker than σ bond electrons. Therefore, the electron densityof the π bonded groups is less than the electron density of the σ bonded ones. For the **BISB** molecule, the electron densitiesof the πbonds in donor (i) groups are calculated at the interval of 1.69569 e-1.88342 e, whereas the electron densities of the σ bonds in donor (i) groups are found between 1.96154 e and 1.98624 e. The electron densities of lone pair n electrons of O, N and Br atoms in donor (i) groups are found between 1.61807 e and 1.97324 e. The electron densities of σ* and π* antibonding bonds in acceptor (j) groups are computed at the intervals0.01427 e-0.05955 e and 0.22630 e-0.39825 e, respectively.The strongest hyperconjugation interaction is from the lone pair n electrons of N17 atom to antibonding π* electrons of C7-N16 bond. This interaction is obtained as n(N17)→π*(C7-N16)[E(2)=50.06 kcal mol^{-1}, ED(i)=1.61807 e, ED(j)=0.39825 e].The n(N18)→σ*(O15-H24) charge transferfor the intramolecular hydrogen bonding in the **BISB** moleculeexhibited a strong hyperconjugation interaction with E(2)=22.38 kcal mol^{-1}, ED(i)=1.87519 e and ED(j)=0.05955 e values.The stabilization energy values for π(C3-C4)→π*(C5-C6), π(C5-C6)→π*(C3-C4), π(C8-N18)→π*(C7-N16), π(C11-12)→π*(C13-C14) and π(C13-C14)→π*(C11-C12) are computedas 32.97 kcal mol^{-1}[ED(i)=1.71814 e, ED(j)=0.33446 e], 17.51 kcal mol^{-1}[ED(i)=1.72682 e, ED(j)=0.30484 e], 20.47 kcal mol^{-1}[ED(i)=1.88342 e, ED(j)=0.39825 e], 16.67 kcal mol^{-1}[ED(i)=1.69569 e, ED(j)=0.35550 e] and21.34 kcal mol^{-1}[ED(i)=1.72424 e, ED(j)=0.30112 e], respectively.Likewise, the σ(C2-N16)→σ*(C7-N18) andσ(C5-C6)→σ*(C1-N17) hyperconjugation interactions are obtainedat 8.54 kcal mol^{-1} [ED(i)=1.97458 e, ED(j)=0.03986 e] and 6.73 kcal mol^{-1} [ED(i)=1.97461 e, ED(j)=0.02405 e] values of stabilization energy, respectively.

4.6. NLO Analysis

The organic, inorganic and organometallic nonlinear optical (NLO) materials have been very attractive in the fields of physics, chemistry and engineering, due to their future potential applications in the optoelectronic and microelectronics such as optical telecommunications, signal processing, optical interconnections, optical computing, optical information processing,sensor protection, optical switching, dynamic image processing and various other photonic technologies [48]. The mean polarizability (α_{total}), the anisotropy of the polarizability ($\Delta\alpha$) and the first hyperpolarizability (β_0) valuesareimportant key parametersto determine NLO properties of the molecules. Therefore, recently, the synthesis and investigations of the novel nonlinear optic materialswith high performance havecreated an interesting study area.

Thepolarizabilities,first hyperpolarizabilities and dipole moments of the **BISB**molecule are calculatedwithB3LYP/6-311G(d,p) level using the finite field approach and they are summarizedin Supplementary Table S2.Thepolarizabilityvalues werecomputed in atomic units (a.u) and theywere transformed using 1 a.u = 0.1482×10^{-24} electrostatic unit (esu) for αvalues and1 a.u = 8.6393×10^{-33} esu for β values. Theμ_{total},α_{total},$\Delta\alpha$ and β_0 valueswere calculatedusing the following equations[49].

$$\alpha_{total} = \frac{1}{3}(\alpha_{xx} + \alpha_{yy} + \alpha_{zz})$$

$$\Delta\alpha = \frac{1}{\sqrt{2}}\left[(\alpha_{xx} - \alpha_{yy})^2 + (\alpha_{yy} - \alpha_{zz})^2 + (\alpha_{zz} - \alpha_{xx})^2 + 6\alpha_{xz}{}^2 + 6\alpha_{xy}{}^2 + 6\alpha_{yz}{}^2\right]^{\frac{1}{2}}$$

$$\beta_0 = \left[(\beta_{xxx} + \beta_{xyy} + \beta_{xzz})^2 + (\beta_{yyy} + \beta_{yzz} + \beta_{yxx})^2 + (\beta_{zzz} + \beta_{zxx} + \beta_{zyy})^2\right]^{\frac{1}{2}}$$

$$\mu_{total} = (\mu_x^2 + \mu_y^2 + \mu_z^2)^{\frac{1}{2}}$$

The dipole moment valuescalculated forthe **BISB** moleculeare-1.5701 Debye for μ_x, 2.5335 Debye for μ_y, 0.1947 Debye for μ_z and 2.9869 Debye for μ_{total}.Theα_{total} and $\Delta\alpha$values are found as 355.1613×10^{-25} and 478.4220×10^{-25} esu, respectively. The calculatedvalue for theβ_0 is found as 92.1329117×10^{-31} esu. In NLO studies, urea is one of the prototypical molecules. Hence, the NLO properties of the molecules can beusually compared with those urea. The calculated values for urea atB3LYP/6-311G(d,p) level are41.4969×10^{-25} esu for α_{total}, $24,5049\times10^{-25}$ esu for $\Delta\alpha$and 3.3014×10^{-31} esu for β_0. The mean polarizability, the anisotropy ofthe polarizability and first hyperpolarizability values of the **BISB** molecule are approximately8.559, 19.524 and 126.192 times greater than those of urea, respectively.

4.7. MEPSurface Analysis

The molecular electrostatic potential (MEP) is widely used as a method for mapping electrostatic potential onto the iso-electron density surface. MEP was established extensively as a helpful quantity to explain the hydrogen bonding, chemical reactivity, presence of intra- and inter-molecular interactions, electronegativity and structure activity of molecule [50]. Three-dimensional charge distribution of MEP is very useful that the negative electrostatic potential regions can be regarded as nucleophilic centers, whereas the positive ones are potential electrophilic sites. Moreover, the electrostatic potential makes the polarization of the electron density visible [64]. An electron density isosurface mapped with electrostatic potential surface depicts the size, shape and charge density of a molecule.

The MEP surface and its contours were simulated with B3LYP/6-311G(d,p) level in order to determine the chemically reactive electrophilic and nucleophilic sites of the **BISB** molecule. They

are given in Fig. 7. As seen from Fig. 7, the possible electrophilic sites or the negative electrostatic potential regions are mainly placed around the O15 and N16 atoms, whereas the nucleophilic sites or the positive ones are localized around the H29 atom and other hydrogen atoms. The calculated values of electron densities on the O15, N16 and H29 atoms are obtained as -2.747, -3.704 (the deepest negative) on MEP surface of the **BISB** molecule and 6.324 a.u. (the highest positive), respectively.

4.8. Atomic Charges

Mulliken atomic charges arise from Mulliken population analysis [51]. Mulliken analysis is the most common, oldest and simplest population analysis method that can be used to characterize the electronic partial charge distribution of atoms in a molecular system. Atomic charges can relate to the electronic structural properties and molecular behavior and reactivity of a molecules. Thus, atomic charges play an important role in quantum chemistry computation. The Mulliken, APT (atomic polar tensor) and NBO atomic charges of the **BISB** molecule were calculated using B3LYP/6-311G(d,p) level and they are given in Supplementary Table S3. As seen from Supplementary Table S3, all hydrogens have positive charges. It is clear that the H23 and H24 atoms have more positive atomic charge than other hydrogens due the electronegativity property of the oxygen and nitrogen atoms. The computed Mulliken, APT and NBO atomic charge values for these hydrogens are 0.2598, 0.3796 and 0.4979 a.u. for H23 atom and 0.2351, 0.2418 and 0.4126 a.u. for H29 one, respectively. The charges of the carbon atoms were computed as either positive or negative at the interval -0.2197 - 0.5068 for Mulliken atomic charges, -0.4980 - 0.7018 a.u. for APT ones and -0.2430 - 0.5823 a.u. for NBO ones. The C7, C8 and C10 carbon atoms which are connected to electronegative O and N atoms belong to more positive atomic charge values. Especially, C7 atom has more positive charge than others due to bonded three negative N atoms. The computed Mulliken, APT and NBO atomic charge values for these carbon atoms were found as 0.5068, 0.7018 and 0.5823 a.u. (for C7 atom), 0.2442, 0.7126 and 0.1826 a.u. (for C8 atom) and 0.2313, 0.4386 and 0.3937 a.u. (for C10 atom), respectively. The Mulliken, APT and NBO atomic charges for the electronegative O15, N16, N17 and N18 atoms were computed as -0.3502, -0.6640 and -0.6672 a.u., -0.3642, -0.4364 and -0.5328 a.u., -0.4595, -0.3455 and -0.5490 a.u. and -0.5048, -0.6865 and -0.5851 a.u., respectively. The Br19 atom was computed at -0.0250 a.u. value for Mulliken atomic charges, -0.2549 a.u. value for APT ones and 0.0525 a.u. value for NBO ones.

4.9. Thermodynamic Properties

Some of the thermodynamic parameters such as thermal energy, heat capacity, entropy, rotational constants and temperature and zero-point vibrational energy (ZPVE), etc.were computed

with B3LYP/6-311G(d,p) level at room temperature of 298.15 K, under 1 atm pressure and in vacuum for the **BISB** and they werelisted in Supplementary Table S4. The partition function which is called as the statical characteristics of a system in thermodynamic equilibrium is very important for thermodynamic parameters. The partition function has four species as to be the translational partition function, electronic one, vibrational one and rotational one. Thepartition functions can be used to compute thermodynamicvariables (such as heat capacity, entropy, equilibrium constants, total energy, free energy, pressure, thermal energy and rate constants, etc.) of a system. Accordingly, it is well known that the total energy of any a molecular system is the sum of electronic,vibrational, rotational and translation energies(or $E = E_e + E_v + E_r + E_t$). The computed minimum total energy (E(RB3LYP)) valuesforthe **BISB** moleculewas found as -3353.34936242 Hartrees. The ZPVE value was computed as 134.90579 kcal/mol. As seen from Supplementary Table S4, the computed value of total thermalenergy was found as144.309 cal/mol×K. The major contribution to thermal energy is came from vibrational energywith 142.531 cal/mol×K value, whereas the minor portions are belonged to electronic enegry with 0.000 cal/mol×K value, transitional and rotational energies with 0.889 cal/mol×K one.Likewise, the calculated heatcapacity (C_v) and entropy (S) valuesare obtained as 58.977and127.264 cal/mol×K, respectively. The electronic, translational, rotational and vibrational energy cantributions to heat capacity and entropy are found as 0.000, 2.981, 2.981 and 53.015 cal/mol×K for heat capacity and 0.000, 43,138, 35.109 and 49.017 cal/mol×K for entropy, respectively. The computed rotational temperatures (Kelvin) and rotational constants (GHz) for the **BISB** molecule werefound as 0.04137, 0.00450 and 0.00405 K and 0.86199, 0.09366 and 0.08448 GHz, respectively.

5. Conclusions

The structural, spectral, electronic, nonlinear optical and thermodynamic characterizations of the synthesized 2-[(1*H*-benzimidazol-2-ylimino)methyl]-4-bromophenol (**BISB**) compound were performed using both experimental and computationalprocedures. The vibrational frequencies, ^{1}H and ^{13}C NMR chemical shifts and UV-Vis. electronic absorption wavelengths were computed and the obtained calculation results were compared with experimental data.The HOMO-LUMO analyses and some chemical properties depending on them, NLO properties, atomic charges, MEP surface analysis and thermodynamic properties weretheoretically investigated for the **BISB** molecule. The potential energy surface (PES)was obtaineddepending on the C8-N18-C7-N16torsional angle. There are three points, namelyone global minimum (conformer 1; 0.0°), one local minimum (conformer 2; 166.0°) and one global maximum (conformer 3;104.0°) on the PES surface. The one imaginary frequency valuecalculated for conformer 3 shows that it is atransition state for the **BISB** molecule. The imaginary frequency for the other two conformers was not

computed. Due to intramolecular hydrogen bonding interaction in the **BISB** molecule, the positions of the OH stretching band at 3238 $cm^{-1}$and proton NMR chemical shifts at 12.81 ppm and 12.03 ppm of the OH hydrogen were investigated using experimental and calculation methods. The n(N18)→σ*(O15-H24) intramolecular charge transfer with the stabilization energy value ofE(2)=22.38 kcal mol^{-1}in the **BISB** molecule was determined by via NBO analysis.The strongabsorption wavelengts observed below 400 nm in experimental UV-Vis. spectrum indicate the enol-imine form of the **BISB** molecule. Likewise, the observed absorption wavelength at 245 nm supports intramolecular hydrogen bonding interaction with the n→σ* transition. According to NLO analysis,the **BISB** moleculesignificantlyexhibited polarizability and first hperpolarizability properties when compared with those of urea and itcan be used as an effective NLO material.

References

[1] S. Som, Schiff bases of benzimidazole analogues: synthesis, characterization andbiological activity, Am. J. Pharm. Health Res. 3 (2015) 192-199.

[2] N. Singh, A. Pandurangan, K. Rana, P. Anand, A. Ahamad, A.K. Tiwari, Benzimidazole: A short review of their antimicrobial activities, Int. Curr. Pharm. J. 1 (2012) 119-127.

[3] E.R. Cole, G. Crank, A. Salam-Sheikh, Antioxidant properties of benzimidazoles, J. Agric. Food Chem. 22 (1974) 918-918.

[4] B. Nandha, L.V.G. Nargund, S.L. Nargund, Design and synthesis of some new imidazole and 1,2,4-triazole substituted fluorobenzimidazoles for antitubercular and antifungal activity, Der Pharma Chemica 5 (2013) 317-327.

[5] S. Gupta, S.S. Pancholi, M.K. Gupta, Synthesis and antimicrobial screening of some acid chloride derivatives of 2-substituted benzimidazoles, Oriental J. Chem. 25 (2009) 219-222.

[6] A.S.A. El-All, F.A.F. Ragab, A.A. Magd El-Din, M.M. Abdalla, M.M. El-Hefnawi, A.A. El-Rashedy, Design, synthesis and anticancer evaluation of some selected schiff bases derived from benzimidazole derivative, Global J. Pharmacol. 7 (2013) 143-152.

[7] A. Mobinikhaledi, N. Forughifar, M. Kalhor, An efficient synthesis of Schiff bases containing benzimidazole moiety catalyzed by transition metal nitrates, Turk. J. Chem. 34 (2010) 367-373.

[8] F. Shemirani, A.A. Mirroshandel, M.S. Niasari, R.R. Kozani,Silica gel coated with Schiff's base: synthesis and application as an adsorbent for cadmium, copper, zinc, and nickel determination after preconcentration by flame atomic absorption spectrometry, J. Anal. Chem. 59 (2004) 228-233.

[9] W. Qin, S. Long, M. Panunzio, S. Biondi, Schiff bases: a short survey on an evergreen chemistry tool, Molecules 18 (2013) 12264-12289.

[10] M. Saeedi, Y.S. Beheshtiha, M.M. Heravi, H.A. Oskooie, Synthesis of novel tetrahydro[4,5]imidazo[2,1-b]-chromeno[4,3,2-de] quinazoline and benzothiazol-2-ylaminoxanthenone derivatives, Heterocycles 83 (2011) 1831-1841.

[11] M.J. Frisch, G.W. Trucks, H.B. Schlegel, G.E. Scuseria, et al., Gaussian 09, Revision C.01, Gaussian, Inc., Wallingford CT, 2009.

[12] R. Dennington, T. Keith, J. Millam, GaussView, Version 5, Semichem Inc., Shawnee Mission KS, 2009.

[13] A.D. Becke, Densityfunctional thermochemistry. III. The role of exact exchange, J. Chem. Phys. 98 (1993) 5648-5652.

[14] C. Lee, W. Yang, R.G. Parr, Development of the Colle-Salvetti correlation-energy formula into a functional of the electron density, Phys. Rev. B. 37 (1988) 785-789.

[15] M.H.Jamr'oz, Vibrational Energy Distribution Analysis VEDA4, Warsaw, 2004.

[16] R.D. Johnson III (Ed.), NIST Computational Chemistry Comparison and Benchmark Database, NIST Standard Reference Database, Number 101, Release 18, October 2016, http://cccbdb.nist.gov/.

[17] R. Ditchfield, Self-consistent perturbation theory of diamagnetism, Mol. Phys. 27 (1974) 789-807.

[18] F. London, Théorie quantique des courants interatomiques dans les combinaisons aromatiques, J. Phys. Radium 8 (1937) 397-409.

[19] K. Wolinski, J.F. Himton, P. Pulay, Efficient implementation of the gauge-independent atomic orbital method for NMR chemical shift calculations, J. Am. Chem. Soc. 112 (1990) 8251-8260.

[20] J. Liu, Z. Liu, S. Yuan, 2-[(1H-Benzimidazol-2-yl)iminomethyl]- 4,6-dibromophenol ethanol hemisolvate, Acta Cryst. E69 (2013) o362.

[21] H.-K. Fun, R. Kia, P.R. Raithby, 2-[(E)-(5-Amino-2,3-di-phenyl-quinoxalin-6-yl)imino-meth-yl]-4-bromo-phenol, Acta Cryst. E64 (2008) o1271-o1272.

[22] Ş. Atalay, T.K. Erdem, F. Erşahin, N. Tınkılıç, (E)-4-Bromo-2-[(4-ethylphenyl) iminomethyl]phenol, Acta Cryst. E64 (2008) o92.

[23] H.-P. Diao, T.-J. Sun, W. Liu, 2-[(1,3-Benzothiazol-2-yl)iminomethyl]-4-bromophenol, Acta Cryst. E67 (2011) o1096.

[24] J. Han, H. Lee, F.-M. Tao, Molecular structures and properties of the complete series of bromophenols: density functional theory calculations, J. Phys. Chem. A 109 (2005) 5186-5192.

[25] J.-B. Su, S. Lin, L.-J. Chen, M.-X. Yang, H. Huang, 1,4-Bis(1*H*-benzimidazol-2-yl)benzene methanol monosolvate, Acta Cryst. E67 (2011) o90.

[26] N.B. Colthup, L.H. Daly, E. Wiberley, Introduction to Infrared and Raman Spectroscopy, Academic Press, New York, 1964.

[27] L.J. Bellamy, The Infrared Spectra of Complex Molecules, Wiley, New York, 1975.

[28] R.M. Silverstein, F.X. Webster, Spectroscopic Identification of Organic Compound, John Willey & Sons, New York, 1998.

[29] B.H. Stuart, Infrared Spectroscopy: Fundamentals and Applications, JohnWilley & Sons, England, 2004.

[30] E. Temel, C. Alaşalvar, H. Gökce, A. Güder, Ç. Albayrak, Y.B. Alpaslan, G. Alpaslan, N. Dilek, DFT calculations, spectroscopy and antioxidant activity studies on (E)-2-nitro-4-[(phenylimino)methyl]phenol, Spectrochim. Acta Part A 136 (2015) 534-546.

[31] C. Alaşalvar, M.S. Soylu, A. Güder, Ç. Albayrak, G. Apaydın, N. Dilek, Crystal structure, DFT and HF calculations and radical scavenging activities of (E)-4,6-dibromo-3-methoxy-2-[(3-methoxyphenylimino)methyl]phenol, Spectrochim. Acta Part A 125 (2014) 319-327.

[32] Ü. Ceylan, G. Ö. Tarı, H. Gökce, E. Ağar, Spectroscopic (FT–IR and UV–Vis) and theoretical (HF and DFT) investigation of 2-Ethyl-N-[(5-nitrothiophene-2-yl) methylidene] aniline, J. Mol. Struct. 1110 (2016) 1-10.

[33] S. Subashchandrabose, H. Saleem, Y. Erdogdu, Ö. Dereli, V. Thanikachalam, J. Jayabharathi, Structural, vibrational and hyperpolarizability calculation of (E)-2-(2-hydroxybenzylideneamino)-3-methylbutanoic acid, Spectrochim. Acta Part A 86 (2012) 231-241.

[34] A. Güder, H. Korkmaz, H. Gökce, Y.B. Alpaslan, G. Alpaslan, Isolation, characterization, spectroscopic properties and quantum chemical computations of an important phytoalexin resveratrol as antioxidant component from Vitis labrusca L. and their chemical compositions, Spectrochim. Acta Part A 133 (2014) 378-395.

[35] M. Karabacak, M. Kurt, The spectroscopic (FT-IR and FT-Raman) and theoretical studies of 5-Bromo-salicylic acid, J. Mol. Struct. 919 (2009) 215-222.

[36] E.F. Mooney, The infrared spectra of chloro- and bromobenzene derivatives-I: Anisoles and phenetoles, Spectrochim. Acta Part A19 (1963) 877-887.

[37] E.F. Mooney, The infra-red spectra of chloro- and bromobenzene derivatives-II. Nitrobenzenes, Spectrochim. Acta Part A 20 (1964) 1021-1032.

[38] A. Gupta, S. Bee, N. Choudhary, S. Mishra, P. Tandon, Molecular structure, vibrational spectroscopic, NBO and HOMO-LUMO studies of 2-amino 6-bromo 3-formylchromone, Mol. Simul. 38 (2012) 567-581.

[39] Y. Sert, A.A. Balakit, N. Öztürk, F. Ucun, G.A. El-Hiti, Experimental (FT-IR, NMR and UV) and theoretical (M06-2X and DFT) investigation, and frequency estimation analyses on (E)-3-(4-bromo-5-methylthiophen-2-yl)acrylonitrile, Spectrochim. Acta Part A 131 (2014) 502-511.

[40] V. Krishnakumar, N. Jayamani, R. Mathammal, K. Parasuraman, Density functional theory calculations and vibrational spectra of 2-bromo-4-chloro phenol and 2-chloro-4-nitro phenol, J. Raman Spectrosc. 40 (2009) 1551-1556.

[41] L.G. Wade Jr, Organic Chemistry, Pearson Prentice Hall, New Jersey, 2006.

[42] R.J. Anderson, D.J. Bendell, and P.W. Groundwater, Organic Spectroscopic Analysis, The Royal Society of Chemistry, Sanderland UK, 2004.

[43] H.O. Kalinowski, S. Berger, S. Braun, Carbon-13 NMR Spectroscopy, John Wiley&Sons, Chichester, 1988.

[44] K. Pihlaja, E. Kleinpeter (Eds.), Carbon-13 Chemical Shifts in Structural and Sterochemical Analysis,VCH Publishers, Deerfield Beach, 1994.

[45] K. Fukui, Role of frontier orbitals in chemical reactions, Science 218 (1982) 747-754.

[46] Y.B. Alpaslan, H. Gökce, G. Alpaslan, M. Macit, Spectroscopic characterization and density functional studies of (Z)-1-[(2-methoxy-5-(trifluoromethyl)phenylamino)methylene]naphthalene-2(1H)-one, J. Mol. Struct. 1097 (2015) 171-180.

[47] F. Wienhold, C.R.Landis, Valency and Bonding-A Natural Bond Orbital Donor-Acceptor Perspective, Cambridge University Press, New York, 2005.

[48] H.S. Nalwa, S. Miyata, Nonlinear Optics of Organic Moleculesand Polymers,CRC Press, Boca Raton, Florida,1997.

[49] Ö. Tamer, D. Avcı, Y. Atalay, Synthesis, X-Ray crystal structure, photophysical characterization and nonlinear optical properties of the unique manganese complex with picolinate and 1,10 phenantroline: toward the designing of new high NLO response crystal, J. Phys. Chem. Solids 99 (2016) 124-133.

[50] J.S. Murray, K. Sen, Molecular Electrostatic Potentials Concepts and Applications, Elsevier Science B.V, Amsterdam, The Netherlands, 1996.

[51] R.S. Mulliken, Electronic Population Analysis on LCAO-MO Molecular Wave Functions. I, J. Chem. Phys. 23 (1955) 1833-1840.

Table 1. The experimental and optimized molecular geometric parameters for all conformers of the **BISB** molecule.

Bond lengths (Å)	**X-Ray[a]**	**Conf. 1**	**Conf. 2**	**Conf. 3**	**Bond angles (°)**	**X-Ray[a]**	**Conf. 1**	**Conf. 2**	**Conf. 3**
C1-C2	1.410(7)	1.419	1.416	1.414	C2-C1-C6	122.9(5)	122.5	122.5	122.6
C1-C6	1.393(7)	1.394	1.393	1.392	C2-C1-N17	104.5(4)	104.4	104.6	104.4
C1-N17	1.374(5)	1.380	1.383	1.387	C6-C1-N17	132.6(5)	133.1	132.9	133.0
C2-C3	1.396(6)	1.400	1.400	1.397	C1-C2-C3	118.9(5)	119.6	119.7	119.7
C2-N16	1.381(6)	1.381	1.380	1.390	C1-C2-N16	110.1(4)	110.4	110.5	110.6
C3-C4	1.369(8)	1.387	1.387	1.390	C3-C2-N16	131.0(5)	130.0	129.7	129.8
C3-H25	0.930	1.083	1.083	1.083	C2-C3-C4	118.1(6)	118.1	118.1	118.1
C4-C5	1.380(8)	1.408	1.408	1.405	C2-C3-H25	120.9	120.1	120.0	120.1
C4-H26	0.930	1.084	1.084	1.084	C4-C3-H25	120.9	121.8	121.9	121.8
C5-C6	1.405(7)	1.390	1.391	1.392	C3-C4-C5	123.2(5)	121.5	121.4	121.4
C5-H27	0.930	1.084	1.084	1.084	C3-C4-H26	118.4	119.5	119.6	119.5
C6-H28	0.930	1.084	1.084	1.084	C5-C4-H26	118.4	119.0	119.0	119.1
C7-N16	1.309(5)	1.313	1.312	1.303	C4-C5-C6	120.5(5)	121.5	121.6	121.4
C7-N17	1.342(6)	1.378	1.390	1.382	C4-C5-H27	119.8	119.2	119.2	119.3
C7-N18	1.401(5)	1.383	1.376	1.399	C6-C5-H27	119.8	119.3	119.2	119.2
C8-C9	1.470(6)	1.443	1.445	1.449	C1-C6-C5	116.3(5)	116.8	116.7	116.7
C8-N18	1.268(6)	1.296	1.292	1.287	C1-C6-H28	121.9	122.0	122.1	122.0
C8-H24	0.930	1.092	1.097	1.096	C5-C6-H28	121.9	121.3	121.2	121.2
C9-C10	1.401(6)	1.421	1.423	1.420	N16-C7-N17	114.4(4)	113.0	112.6	113.7
C9-C14	1.370(7)	1.409	1.409	1.408	N16-C7-N18	129.7(4)	128.4	122.6	125.8
C10-C11	1.392(6)	1.400	1.402	1.402	N17-C7-N18	115.9(4)	118.7	124.8	120.5
C10-O15	1.352(6)	1.338	1.334	1.336	C9-C8-N18	121.0(4)	122.1	121.8	122.2
C11-C12	1.373(7)	1.385	1.384	1.384	C9-C8-H24	119.5	118.0	115.9	116.7
C11-H20	-	1.083	1.083	1.083	N18-C8-H24	119.5	119.9	122.3	121.0
C12-C13	1.391(7)	1.400	1.400	1.400	C8-C9-C10	121.4(4)	121.8	121.4	121.3
C12-H21	0.930	1.083	1.083	1.083	C8-C9-C14	119.1(4)	119.0	119.3	119.2
C13-C14	1.386(6)	1.380	1.379	1.380	C10-C9-C14	119.5(4)	119.2	119.3	119.5
C13-Br19	1.891(5)	1.917	1.918	1.917	C9-C10-C11	119.1(5)	119.3	118.9	119.0
C14-H22	0.930	1.083	1.084	1.083	C9-C10-O15	122.4(4)	122.1	122.7	122.6
O15-H23	0.820	0.989	0.991	0.989	C11-C10-O15	118.5(4)	118.6	118.4	118.5
N17-H29	0.860	1.007	1.006	1.007	C10-C11-C12	121.3(4)	120.7	120.9	120.7
H23···N18	1.900	1.755	1.756	1.765	C10-C11-H20	-	118.4	118.1	118.3
O15···N18	2.618(6)	2.642	2.633	2.642	C12-C11-H20	-	121.0	121.0	121.0
RMSD	**-**	**0.088**	**0.088**	**0.087**	C11-C12-C13	119.2(4)	120.0	120.0	120.1
R^2	**-**	**0.96979**	**0.96992**	**0.97070**	C11-C12-H21	120.4	120.0	120.0	119.9
					C13-C12-H21	120.4	120.0	120.0	119.9
					C12-C13-C14	119.9(5)	120.5	120.4	120.4
					C12-C13-Br19	119.9(4)	119.6	119.6	119.6
					C14-C13-Br19	120.2(4)	120.0	119.9	120.0
					C9-C14-C13	121.0(4)	120.4	120.5	120.3
					C9-C14-H22	119.5	119.1	119.2	119.2
					C13-C14-H22	119.5	120.6	120.3	120.4
					C10-O15-H23	109.5	107.3	108.2	108.1
					C2-N16-C7	104.0(4)	105.1	105.4	104.7
					C1-N17-C7	107.0(4)	107.1	106.8	106.6
					C1-N17-H29	126.5	127.9	125.8	127.3
					C7-N17-H29	126.5	125.1	126.8	125.7
					C7-N18-C8	120.3(3)	118.6	123.1	119.7
					O15-H23···N18	146.0	147.3	145.1	145.8
					RMSD	**-**	**0.965**	**1.969**	**1.196**
					R^2	**-**	**0.97989**	**0.91445**	**0.96845**

[a] Taken from Ref [20] and Conf.; Conformer.

Table 2. The computed and experimental vibrational frequencies, their assignments and their symmetry species of the **BISB** molecule.

Sym.	Assignments (PED%)	Exp. (cm^{-1})		The calculated vibrational parameters with B3LYP/6-311(d,p) level							
				Conformer 1				Conformer 2		Conformer 3	
		IR	Raman	Unscaled freq.	Scaled freq.	I_{IR}	S_{Raman}	Unscaled freq.	Scaled freq.	Unscaled freq.	Scaled freq.
A′	νNH(100)	3317	-	3657	3536	61.416	74.088	15	14	-52	-50
A′	νOH(99)	3238	-	3287	3178	387.906	64.650	40	39	36	35
A′	νCH(98) in ring 1	-	-	3206	3100	2.687	244.620	45	43	43	41
A′	νCH(93) in ring 3	-	-	3198	3092	20.653	246.672	99	96	83	80
A′	νCH(95) in ring 1	-	-	3192	3087	0.321	105.153	120	116	119	115
A′	νCH(99) in ring 1	-	-	3191	3086	0.892	2.279	151	146	130	125
A′	νCH(92) in ring 3	-	-	3189	3084	24.614	241.901	183	177	177	171
A′	νCH(99) in ring 3	-	-	3178	3073	8.996	198.610	212	205	217	210
A′	νCH(87) in ring 3	3068	-	3168	3063	0.398	45.951	256	247	239	231
A′	νC_8H_{24}(100)	3030	-	3098	2996	8.107	64.597	268	259	262	253
A′	νCC(51) in ring 3	1620	-	1666	1611	11.988	191.067	272	263	282	273
A′	νCC(39) in ring 1+δHOC(19)	1599	1605	1660	1605	36.689	225.598	305	295	321	310
A′	$\nu N_{18}C_8$(38)+νCC(12) in ring 1+δHCN(10)	1588	-	1641	1587	203.176	4294.597	338	327	335	324
A′	[νCC(23)+δring(13)] in ring 3+δring(10) in ring 2	1561	1567	1621	1567	6.933	152.802	373	361	353	342
A′	νCC(22) in ring 1+δHOC(17)+$\nu N_{18}C_8$(12)+νC_9C_8(10)	-	-	1598	1545	155.917	1597.676	400	387	412	399
A′	$\nu N_{18}C_7$(20)+$\nu N_{16}C_7$(14)+δHNC(12)	1511	1512	1546	1495	118.921	5473.505	416	402	430	415
A′	[νCC(28)+δHCC(24)] in ring 1	1473	-	1520	1470	26.091	734.876	448	433	455	440
A′	[δHCC(28)+νCC(11)] in ring 1+δHOC(20)	-	-	1508	1458	141.199	286.325	468	452	461	446
A′	[δring(20)+δHCC(11)] in ring 1+δHOC(14)	1437	1439	1483	1434	81.245	2206.390	480	465	493	476
A′	δHCC(30) in ring 3+δring(10) in ring 2	-	-	1466	1418	40.777	2803.281	531	514	536	518
A′	δHCC(12) in ring 3+δHOC(11)	1401	-	1451	1404	15.741	1501.712	554	536	541	524
A′	νCC(13) in ring 1+δHNC(11)+$\nu N_{17}C_7$(10)	1367	1378	1425	1378	52.350	801.986	586	567	578	558
A′	νCC(16) in ring 1+$\nu N_{17}C_1$(10)	1340	1337	1401	1355	65.227	105.420	589	569	591	572
A′	δHCN(29)+νCC(14) in ring 3+$\nu N_{16}C_7$(14)	1318	1316	1367	1322	12.272	245.306	629	608	631	610
A′	[νCC(52)+δHCC(10)] in ring 1+δHCN(11)	1301	1308	1347	1303	7.106	713.343	638	617	636	615
A′	[δHCC(39)+νCC(13)] in ring 3	-	-	1331	1287	17.303	259.000	650	629	647	626
A′	νOC(35)+[νCC(12)+δHCC(11)] in ring 1	1266	1277	1315	1272	74.311	24.261	715	692	723	699
A′	$\nu N_{16}C_2$(39)+νCC(11) in ring 3	-	1240	1302	1259	57.800	2320.908	741	717	732	708
A′	[δHCC(51)+νCC(12)] in ring 1	1216	-	1258	1217	34.196	335.987	755	730	754	729
A′	[δHCC(33)+νCC(12)] in ring 3	-	1204	1253	1212	8.055	145.208	767	742	769	743
A′	δHNC(19)+νCC(14) in ring 1+νC_9C_8(13)	1188	1180	1230	1189	113.787	15.330	781	755	781	755
A′	δHNC(23)+δHCC(12) in ring 1+νC_9C_8(10)	1169	1148	1190	1151	78.655	1323.029	804	778	809	782

A′	δHCC(51) in ring 3	1137	-	1170	1131	2.662	917.585	834	806	811	785
A′	[δHCC(55)+νCC(26)] in ring 1	-	1119	1153	1115	6.798	50.007	851	823	844	816
A′	[δHCC(51)+νCC(29)] in ring 3	1102	-	1137	1100	3.924	24.056	861	833	863	834
A′	[νCC(37)+δHCC(30)] in ring 1	1074	1080	1092	1056	16.551	24.822	875	846	871	842
A′	$\nu N_{17}C_1(17)+\nu N_{18}C_7(14)+\delta C_3C_2N_{16}(11)+\delta$ring(10) in ring 2	1030	1038	1055	1020	1.017	7.902	882	853	890	861
A″	τHCNC(91)	-	-	1024	990	5.704	9.338	912	882	908	878
A′	[δring(26)+δHCC(14)+νCC(10)] in ring 3	995	1000	1024	990	8.330	65.775	924	893	925	895
A″	[τHCCC(69)+τring(15)] in ring 3	-	950	984	952	0.066	0.149	944	913	941	910
A″	τHCCC(78) in ring 1	934	-	965	934	0.150	0.285	966	934	970	938
A″	τHCCC(79) in ring 3	915	922	943	912	1.958	0.098	980	947	983	950
A′	δring(38) in ring 1	899	-	927	897	12.443	292.680	985	952	1011	977
A′	δring(37) in ring 3+δring(17) in ring 1	-	-	913	883	0.329	17.956	1009	976	1021	987
A″	τHCCC(71) in ring 1	872	869	891	861	9.128	0.202	1031	997	1039	1005
A′	δring(41) in ring 2+νCC(11) in ring 3	848	-	883	854	2.994	134.331	1092	1056	1093	1057
A″	τHCCC(78) in ring 3	-	832	862	834	0.579	0.748	1136	1098	1133	1096
A″	τHCCC(71) in ring 1+γOCCC(18)	817	817	841	813	12.261	0.561	1153	1115	1153	1115
A″	τHOCC(85)	783	793	814	787	110.909	0.719	1170	1132	1172	1133
A′	[νCC(23)+δring(15)] in ring 1+δOCC(11)	-	-	803	776	9.624	33.002	1209	1169	1195	1155
A″	$\tau C_2N_{16}C_7N_{17}(34)+[\tau$ring(20)+τHCCC(11)] in ring 3+$\gamma C_3C_1N_{16}C_2(18)$	-	752	782	756	5.764	0.614	1221	1181	1221	1180
A′	δring(10) in ring 1+δring(10) in ring 2	739	737	768	743	24.499	16.071	1252	1211	1247	1206
A″	τHCCC(70) in ring 3	-	-	757	732	62.850	0.032	1257	1215	1259	1217
A″	τHCCC(23) in ring 3+γNNNC(21)+γOCCC(10)	-	-	742	717	5.396	1.007	1297	1254	1286	1244
A″	τHCCC(25) in ring 1+γOCCC(19)+γNNNC(13)	702	692	716	693	1.981	2.181	1321	1277	1320	1276
A′	δring(28) in ring 1	643	632	652	631	22.912	5.436	1330	1287	1324	1281
A′	δring(47) in ring 1+νBrC(13)	624	-	638	617	17.617	10.861	1350	1306	1349	1305
A′	δring(54) in ring 3+δring(27) in ring 2	603	607	629	608	4.700	14.896	1381	1335	1377	1331
A″	[τring(33)+τHCCC(14)] in ring 3+$\gamma C_3C_1N_{16}C_2(29)$	570	587	589	570	1.625	0.030	1389	1343	1388	1342
A′	$\delta N_{17}C_7N_{16}(25)+\delta$ring(20) in ring 3	-	-	581	562	21.769	32.130	1419	1372	1422	1375
A″	[τring(42)+τHCCC(15)] in ring 3+γBrCCC(13)	547	527	555	537	14.319	0.110	1427	1380	1434	1387
A′	δring(23) in ring 3+$\delta C_3C_2N_{16}(18)+\delta$ring(13) in ring 1	507	511	529	512	4.603	23.323	1465	1416	1473	1425
A″	τHNCC(60)+γNNNC(11)	-	493	498	482	54.924	0.530	1476	1427	1479	1430
A′	δOCC(56)+δCCC(10) in ring 1	464	467	469	453	12.450	0.758	1502	1452	1504	1454
A″	τring(26) in ring 1+τHNCC(25)+γOCCC(11)	-	457	468	452	32.238	0.164	1521	1471	1520	1469
A″	$\gamma C_6N_{17}C_2C_1(51)$	435	427	444	429	0.177	0.359	1554	1502	1573	1521
A′	$\delta C_{14}C_9N_{18}(23)+\delta C_3C_2N_{16}(14)$	-	414	411	397	1.690	2.932	1599	1546	1603	1550
A″	τring(38) in ring 3+τring(14) in ring 2+γNNNC(11)	-	368	375	363	0.736	0.364	1622	1568	1626	1572
A″	τring(47) in ring 1+γOCCC(18)+γBrCCC(15)	-	349	343	332	0.324	2.536	1651	1597	1657	1603

A′	νBrC(29)+δring(12) in ring 1	-	302	302	292	0.830	3.596	1658	1603	1668	1613
A″	$\gamma C_{14}C_9C_8N_{18}$(36)+γBrCCC(25)	-	272	277	268	7.963	1.474	1668	1613	1680	1624
A′	νBrC(23)+δBrCC(23)	-	-	269	260	4.011	7.416	3030	2930	3051	2950
A″	$\gamma C_6N_{17}C_2C_1$(33)+τring(29) in ring 2+$\tau C_5C_6C_1N_{17}$(15)	-	240	257	249	0.651	0.660	3167	3063	3166	3062
A″	τring(25) in ring 3+$\tau C_{16}C_8N_{18}C_7$(20)+τring(12) in ring 1+$\gamma C_3C_1N_{16}C_2$(11)	-	215	221	213	1.518	0.953	3177	3072	3176	3071
A′	$\delta C_9C_8N_{18}$(16)+νC_9C_8(13)+$\nu N_{18}C_7$(12)	-	191	185	179	1.241	0.491	3185	3080	3188	3083
A′	δBrCC(43)+$\delta N_{18}C_7N_{16}$(14)+$\delta C_{14}C_9C_8$(13)	-	-	150	145	1.071	2.229	3188	3083	3188	3083
A″	τring(71) in ring 1	-	-	120	116	0.155	5.523	3193	3087	3193	3088
A″	Lattice mode	-	-	99	96	1.868	2.193	3199	3094	3197	3092
A′	Lattice mode	-	-	46	44	0.008	5.309	3207	3101	3207	3101
A″	Lattice mode	-	-	42	41	0.002	0.997	3264	3156	3290	3182
A″	Lattice mode	-	-	27	26	2.636	3.917	3663	3542	3657	3537
	RMSD	**36.251**	**9.904**								
	R^2	**0.99767**	**0.99950**								

ν, stretching; δ, in-plane bending; τ, torsion; γ, out-of-plane bending; I_{IR}, IR intensity (km/mol); S_{Raman}, Raman scattering activity ($Å^4$/amu); TED, total energy distribution.

Table 3. The experimental and computed ^{1}H and ^{13}C NMR isotropic chemical shifts (with recpect to TMS, all values in ppm) of the **BISB** molecule.

Atoms	**$\delta_{exp.}$ (in DMSO-d_6)**	**$\delta_{cal.}$ (in vacuum)**	**$\delta_{cal.}$ (in DMSO)**
C1	132.86	137.00	137.76
C2	142.29	147.65	147.22
C3	118.75	124.39	122.70
C4	121.66	126.69	126.80
C5	122.05	127.16	127.32
C6	110.57	111.51	114.04
C7	153.86	154.93	156.18
C8	159.41	167.69	168.25
C9	119.28	123.24	123.81
C10	163.12	168.40	168.37
C11	111.33	121.82	122.23
C12	136.73	141.96	142.59
C13	122.45	132.78	131.90
C14	134.06	140.63	141.38
RMSD	**-**	**6.156**	**6.312**
R^2	**-**	**0.97361**	**0.98031**
H20	7.01-8.09	6.91	7.06
H21	7.01-8.09	7.34	7.52
H22	7.01-8.09	7.44	7.64
H23	12.81 and 12.03	12.29	12.68
H24	9.63	9.76	9.71
H25	7.01-8.09	7.83	7.83
H26	7.01-8.09	7.35	7.47
H27	7.01-8.09	7.30	7.46
H28	7.01-8.09	7.31	7.64
H29	7.01-8.09	7.60	8.44

Table 4. The computed and experimental UV-Vis. parameters of the **BISB** molecule (in vacuum/chloroform).

Exp. λ (nm)	Transitions	The calculated with B3LYP/6-311G(d,p) level				
		$\lambda_{max.}$ (nm)	Major transition	Major contribution	Excitation energy (eV)	*f* (oscillator strength)
386	π→π*	387.09/394.45	H→L	0.68732/0.69817	3.2030/3.1432	0.6336/0.8274
353	π→π*	341.80/341.98	H-2→L	0.68275/0.68608	3.6274/3.6255	0.2331/0.2166
278	π→π*	263.92/264.50	H-3→L	0.55614/0.58515	4.6978/4.6875	0.1517/0.1793
		244.77/244.54	H→L+2	0.51207/0.56098	5.0653/5.0701	0.1768/0.1441
245	n→σ*	221.17/220.87	H-2→L+1	0.48338/0.44281	5.6058/5.6134	0.0630/0.1083
		216.47/217.49	H-1→L+2	0.47389/0.42760	5.7276/5.7008	0.3288/0.3478
		203.39/204.44	H→L+4	0.48833/0.53020	6.0959/6.0645	0.0885/0.1282

Table 5. The computed results with second order perturbation theory of Fock matrix in NBO of the **BISB** molecule.

ED(i)(e)	Donor (i)	ED(j)(e)	Acceptor (j)	E(2)[a] (kcal/mol)	E(j)-E(i)[b] (a.u.)	F(i,j)[c] (a.u.)
1.96568	σ(C1-C2)	0.02272	σ*(C1-C6)	5.04	1.24	0.071
1.96568	σ(C1-C2)	0.01724	σ*(N17-H29)	4.69	1.06	0.063
1.97481	σ(C1-C6)	0.04143	σ*(C1-C2)	4.97	1.24	0.070
1.97458	σ(C2-N16)	0.03986	σ*(C7-N18)	8.54	1.22	0.091
1.97695	σ(C3-C4)	0.01986	σ*(C2-N16)	5.17	1.17	0.070
1.71814	π(C3-C4)	0.33446	π*(C5-C6)	20.15	0.28	0.068
1.97809	σ(C3-H25)	0.04143	σ*(C1-C2)	4.39	1.04	0.060
1.97856	σ(C4-H26)	0.02463	σ*(C2-C3)	4.01	1.08	0.059
1.97856	σ(C4-H26)	0.01427	σ*(C5-C6)	4.03	1.09	0.059
1.97461	σ(C5-C6)	0.02405	σ*(C1-N17)	6.73	1.14	0.078
1.72682	π(C5-C6)	0.30484	π*(C3-C4)	17.51	0.29	0.065
1.97842	σ(C5-H27)	0.02272	σ*(C1-C6)	4.00	1.08	0.059
1.97911	σ(C6-H28)	0.04143	σ*(C1-C2)	4.34	1.05	0.061
1.98334	σ(C7-N16)	0.02463	σ*(C2-C3)	5.48	1.42	0.079
1.84140	π(C7-N16)	0.22630	π*(C8-N18)	6.67	0.30	0.041
1.98571	σ(C7-N17)	0.02272	σ*(C1-C6)	4.93	1.39	0.074
1.97094	σ(C8-C9)	0.03986	σ*(C7-N18)	4.49	1.14	0.064
1.88342	π(C8-N18)	0.39825	π*(C7-N16)	20.47	0.35	0.082
1.98624	σ(C8-H24)	0.04002	σ*(C9-C10)	4.34	1.06	0.061
1.97369	σ(C9-C10)	0.02281	σ*(C9-C14)	4.05	1.24	0.063
1.96154.	σ(C9-C14)	0.02511	σ*(C13-C14)	4.35	1.28	0.067
1.96154	σ(C9-C14)	0.03468	σ*(C13-Br19)	5.60	0.79	0.059
1.96871	σ(C11-C12)	0.02791	σ*(C12-C13)	4.01	1.26	0.064
1.96871	σ(C11-C12)	0.03468	σ*(C13-Br19)	5.26	0.80	0.058
1.69569	π(C11-C12)	0.35550	π*(C13-C14)	16.67	0.28	0.062
1.97521	σ(C11-H20)	0.04002	σ*(C9-C10)	4.40	1.04	0.061
1.97521	σ(C11-H20)	0.02791	σ*(C12-C13)	4.16	1.07	0.060
1.97713	σ(C12-H21)	0.02511	σ*(C13-C14)	4.42	1.11	0.062
1.72424.	π(C13-C14)	0.30112	π*(C11-C12)	21.34	0.30	0.072
1.97648	σ(C14-H22)	0.04002	σ*(C9-C10)	4.51	1.04	0.062
1.97648	σ(C14-H22)	0.02791	σ*(C12-C13)	4.53	1.08	0.062
1.98596	σ(O15-H23)	0.02487	σ*(C10-C11)	5.22	1.29	0.073
1.97324	n(O15)	0.04002	σ*(C9-C10)	7.68	1.09	0.082
1.91492.	n(N16)	0.04143	σ*(C1-C2)	6.72	0.89	0.070
1.91492	n(N16)	0.04948	σ*(C7-N17)	9.94	0.79	0.080
1.91492	n(N16)	0.03986	σ*(C7-N18)	2.14	0.81	0.038
1.61807	n(N17)	0.39825	π*(C7-N16)	50.06	0.28	0.106
1.87519	n(N18)	0.02373	σ*(C7-N16)	9.54	0.94	0.087
1.87519	n(N18)	0.02932	σ*(C8-H24)	9.31	0.79	0.078
1.87519	n(N18)	0.05955	σ*(O15-H23)	22.38	0.78	0.120
1.94462	n(Br19)	0.35550	π*(C13-C14)	9.42	0.31	0.052

ED is the electron density.
[a] E(2) is the energy of hyperconjugative interaction.
[b] Energy difference between donor (i) and acceptor (j) NBO.
[c] F(i,j) is the Fock matrix element between i and j NBO.

Figure 1. The optimized molecular structure of the **BISB** molecule.

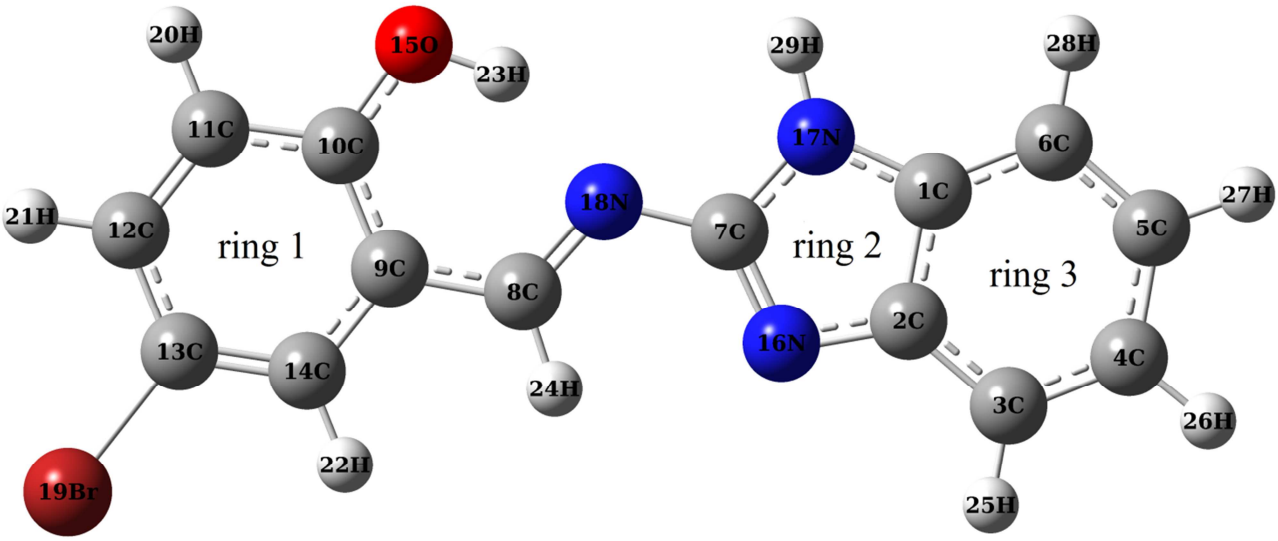

Figure 2. The potential energy surface around C8-N18-C7-N1 dihedral angle of the **BISB** molecule.

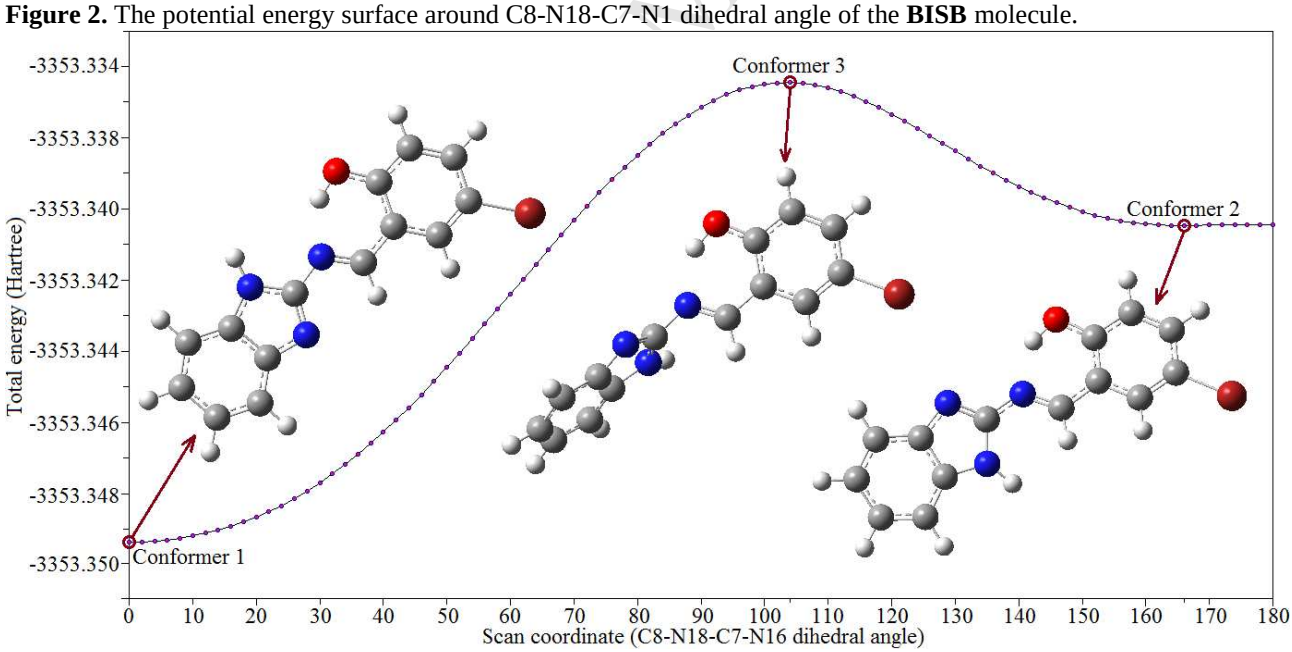

Figure 3. Experimental ((b) and (c)) and simulated ((a) and (d)) IR and Raman spectra of the **BISB** molecule.

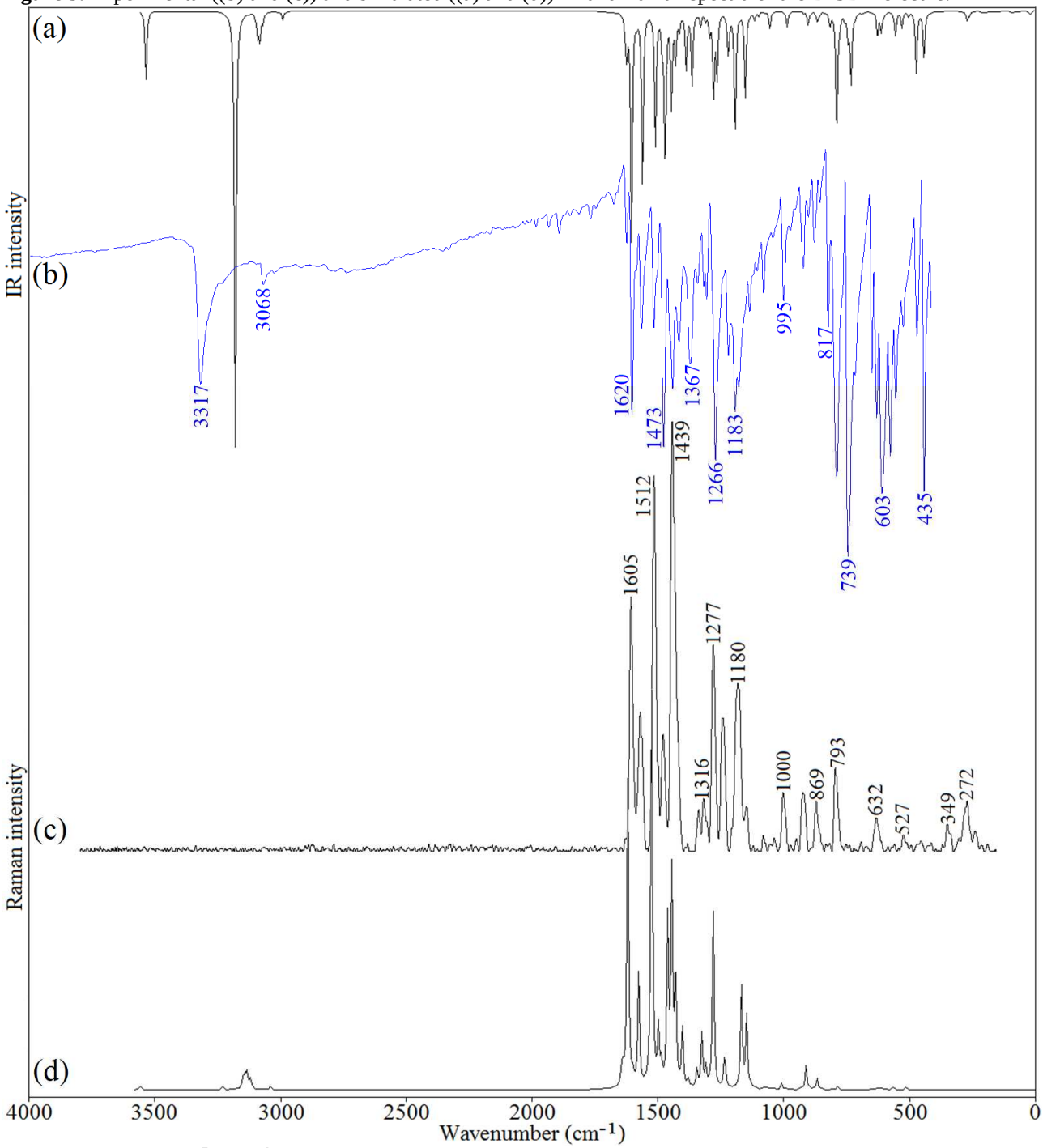

Figure 4. Experimental ^{13}C (top) and ^{1}H (bottom) NMR chemical shift spectra of the **BISB** molecule.

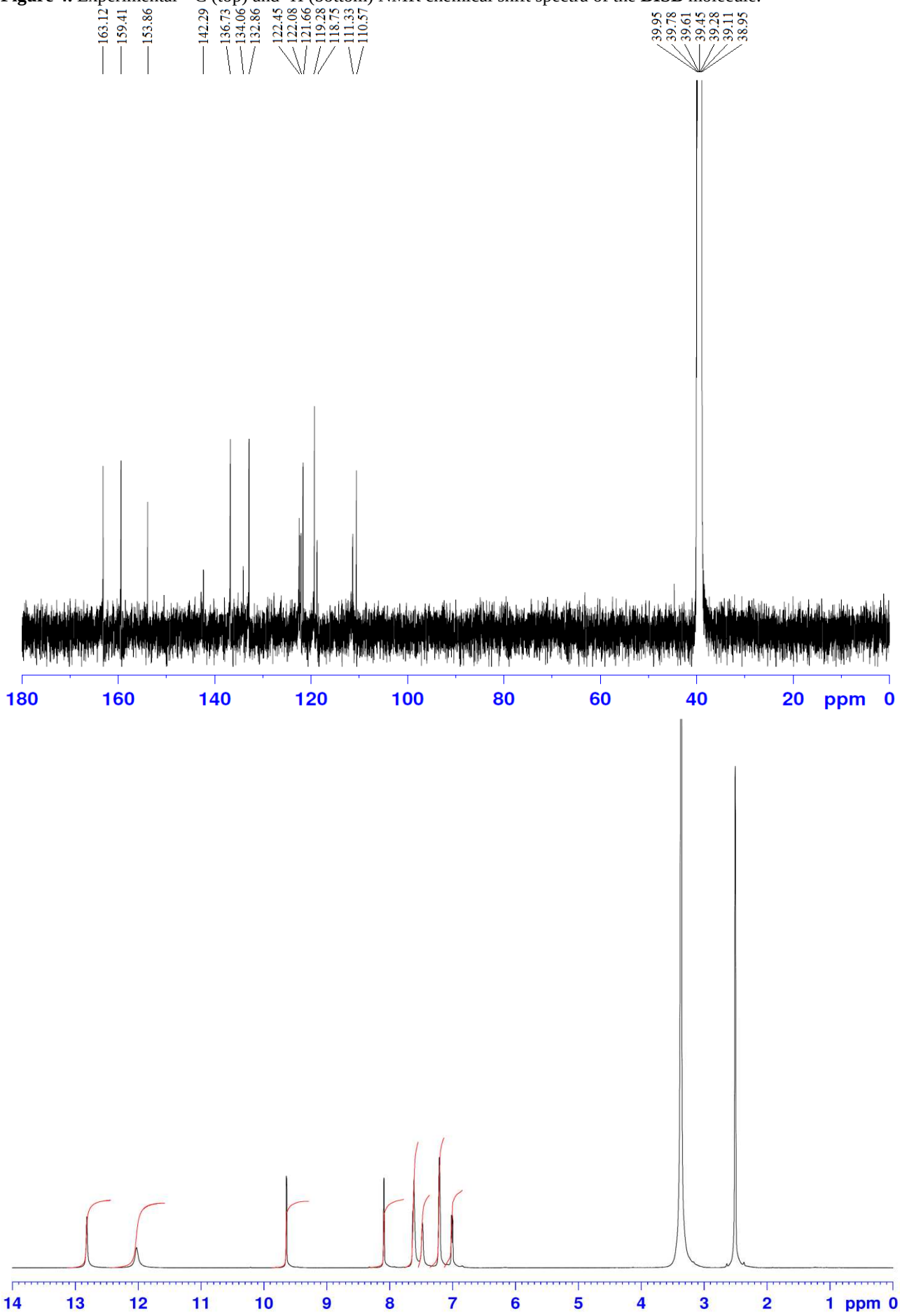

Figure 5 The molecular orbital surfaces and their energy values of the **BISB** molecule (vacuum/chloroform).

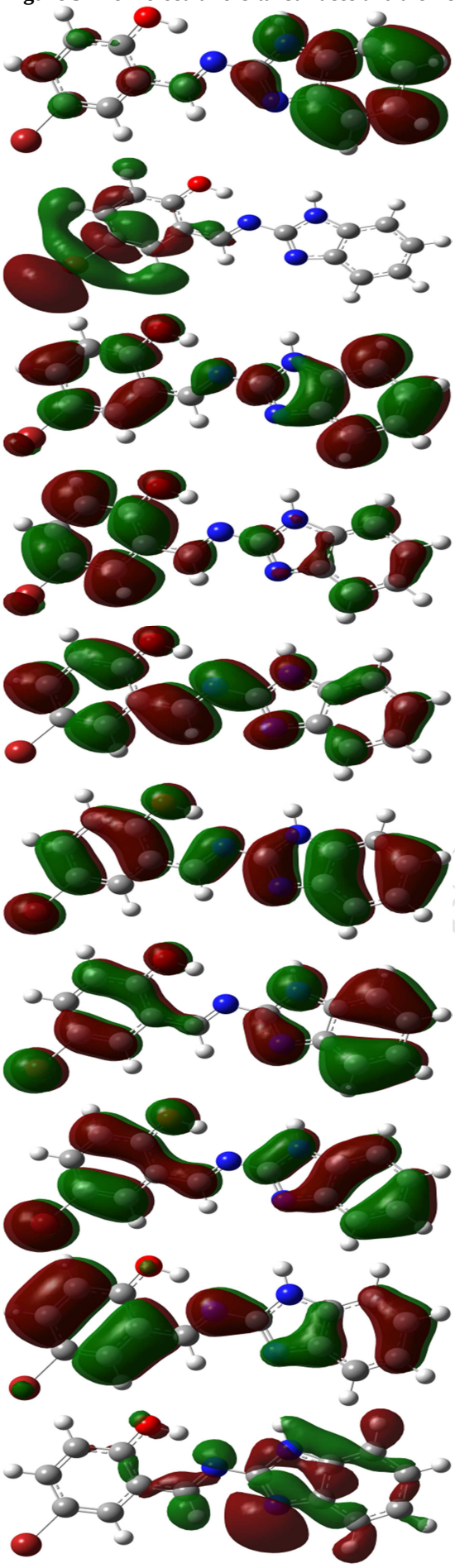

E(LUMO+4)=0.184 eV / 0.177 eV

E(LUMO+3)=-0.380 eV / -0.420 eV

E(LUMO+2)=-0.462 eV / -0.469 eV

E(LUMO+1)=-0.639 eV / -0.628 eV

E(LUMO)=-2.551 eV / -2.526 eV

E(HOMO)=-6.069 eV / -6.086 eV

E(HOMO-1)=-6.542 eV / -6.550 eV

E(HOMO-2)=-6.623 eV / -6.639 eV

E(HOMO-3)=-7.777 eV / -7.760 eV

E(HOMO-4)=-7.908 eV / -7.983 eV

Figure 6. Experimental (a), simulated (in chloroform (b) and vacuum (c)) UV-Vis. spectra of the **BISB** molecule.

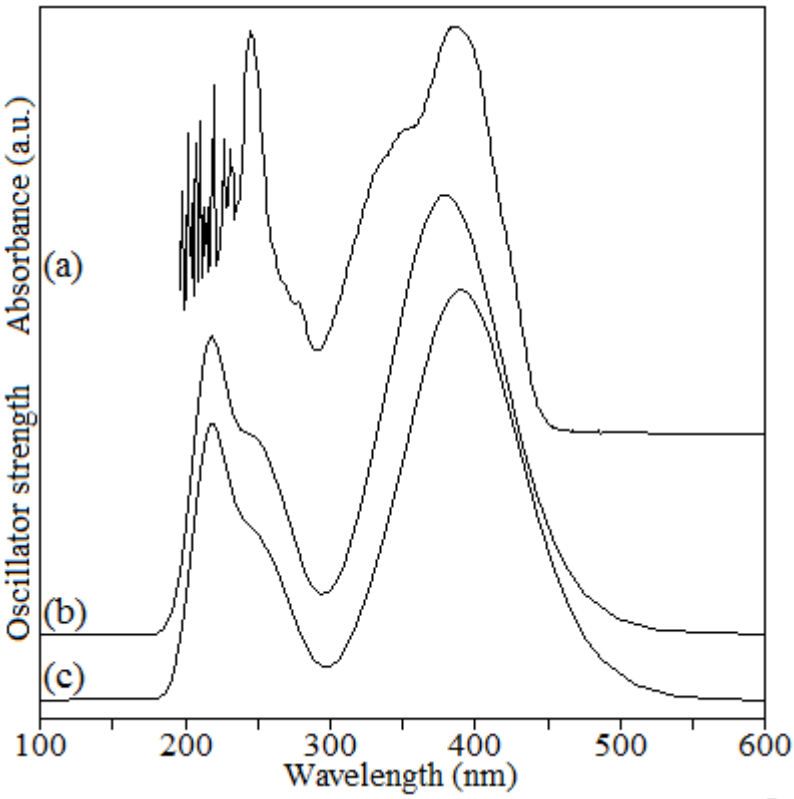

Figure 7. The MEP (top) and its contour (bottom) surfaces of the **BISB** molecule.

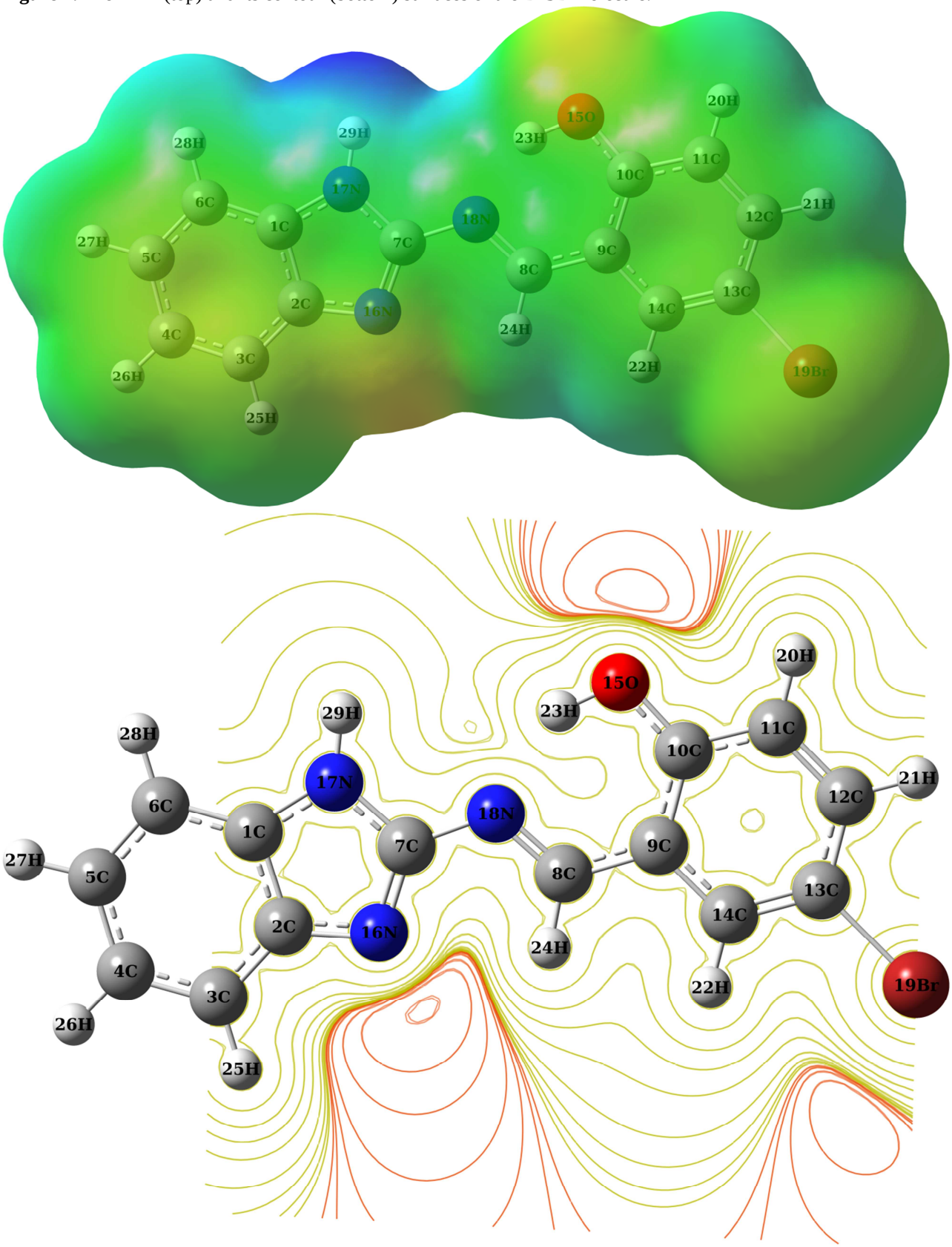

Highlights

- Molecular conformational and intramolecular hyrogen bonding (O-H···N) analyses
- FT-IR, Raman, NMR and UV-Vis. spectroscopic investigations
- DFT/B3LYP/6-311G(d,p) computations
- NLO and thermodynamic properties
- Atomic charge, MEP, NBO and HOMO-LUMO analyses